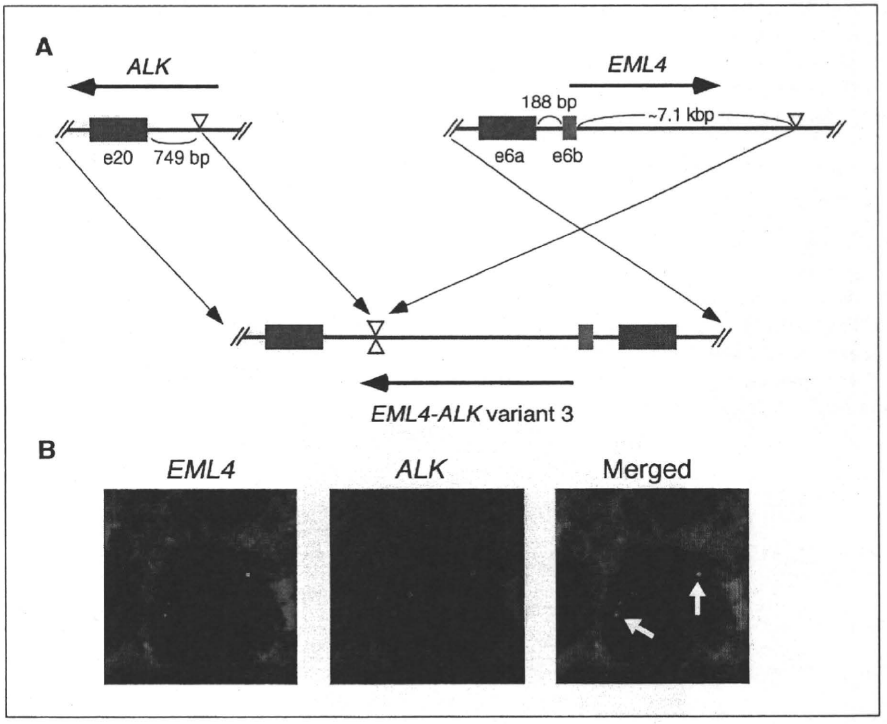

Figure 2. Chromosomal rearrangement responsible for generation of *EML4-ALK* variant 3. *A*, schematic representation of the chromosomal rearrangement underlying the generation of *EML4-ALK* variant 3. Exon 6b of *EML4* is located 188 bp downstream of exon 6a. In NSCLC specimen ID no. 7969, *EML4* is disrupted at a position ~7.1 kbp downstream of exon 6b and is ligated to a position 749 bp upstream of exon 20 of *ALK*, giving rise to the *EML4-ALK* (variant 3) fusion gene. *Horizontal arrows*, direction of transcription. *B*, FISH analysis of a representative cancer cell in a histologic section of lung adenocarcinoma (ID no. 7969) with differentially labeled probes for *EML4* (*left*) and *ALK* (*center*). Two fusion signals (*arrows*) and a pair of green (corresponding to *EML4*) and red (corresponding to *ALK*) signals are present in the merged image (*right*).

The cDNA for FLAG-tagged EML4-ALK variant 3b was also inserted into pMX-iresCD8 for the expression of both EML4-ALK and mouse CD8 (8), and the resulting recombinant retroviruses were used to infect mouse BA/F3 cells (9). CD8-positive cells were then purified with the use of a miniMACS magnetic bead–based separation system (Miltenyi Biotec) and cultured in the absence or presence of mouse interleukin-3 (IL-3; Sigma) or 2,4-pyrimidinediamine (Example 3-39, a specific inhibitor of ALK enzymatic activity that was developed by Novartis[6] and synthesized by Astellas Pharma).

Mouse 3T3 fibroblasts and NCI-H2228 lung cancer cells (both from American Type Culture Collection) as well as 3T3 cells expressing v-Ras were plated in 96-well spheroid culture plates (Celltight Spheroid, Sumilon) at a density of 1×10^3 per well. Cell growth was examined with the WST-1 Cell Proliferation Reagent (Clontech) after culture for 5 d with 2,4-pyrimidinediamine.

Luciferase reporter assays. The promoter fragments of *Fos*, *Myc*, and *Bcl-x_L* genes were ligated to a luciferase cDNA to generate pFL700 (10), pHXLuc (11), and pBclxl-Luc (12) reporter plasmids, respectively. Luciferase cDNA ligated to the DNA binding sequence for nuclear factor κB (NF-κB) or to the GAS sequence was obtained from Stratagene. HEK293 cells were transfected with these various reporter plasmids together with the expression plasmid for EML4-ALK variant 3b or the empty vector, as described previously (13). The pGL4 plasmid (Promega) for expression of *Renilla* luciferase was also included in each transfection mixture. After culture of the cells for 2 d, luciferase activity in cell lysates was measured with a Luciferase Assay system (Promega).

Results and Discussion

Detection of *EML-ALK* variant 3. The EML4-ALK variant 1 and 2 proteins are produced as a result of genomic rearrangements that lead to the juxtaposition of exons 13 and 20 of *EML4*, respectively, to exon 20 of *ALK*. It is theoretically possible that exon 2, 6, 18, or 21 of *EML4* also could undergo in-frame fusion to exon 20 of *ALK*. We therefore examined whether transcripts of any such novel *EML4-ALK* fusion genes are present in NSCLC cells by RT-PCR analysis with primers that flank each putative fusion point (data not shown). With the primer set for amplification of the *EML4* (exon 6)-*ALK* (exon 20) fusion cDNA, we detected a pair of PCR products in two individuals with lung adenocarcinoma (Fig. 1*A*). Although one of the patients (tumor ID no. 7969) had a smoking index of 540, the other patient (tumor ID no. 2075) had never smoked. Nucleotide sequencing of each PCR product from both patients revealed that the smaller product of 515 bp corresponded to a fusion cDNA linking exon 6 of *EML4* to exon 20 of *ALK*, whereas the larger product of 548 bp contained an additional sequence of 33 bp that was located between these exons of *EML4* and *ALK* and which mapped to intron 6 of *EML4* (Fig. 1*B*). The larger cDNA would thus be expected to encode a fusion protein with an insertion of 11 amino acids between the EML4 and ALK sequences of the protein encoded by the smaller cDNA.

Although we did not detect human mRNAs or expressed sequence tags containing this cryptic exon of *EML4* in the nucleotide sequence databases, it is likely that this exon is physiologic and functional because (*a*) the fusion cDNA containing this exon was identified in two independent patients and in amounts no less than those of the corresponding cDNA without it (Fig. 1*A*); (*b*) the intron-exon boundary sequence for this exon conforms well to the AG-GU rule for mRNA splicing (Fig. 1*B*); and (*c*) *EML4* cDNAs or expressed sequence tags containing this exon were detected in the sequence databases for other species (for instance, GenBank accession no. AK144604 corresponding to a mouse *EML4* cDNA). We thus refer to this cryptic exon as exon 6b and to the original exon 6 as exon 6a (Fig. 1*B*). The novel isoforms of *EML4-ALK* transcripts containing exons 1 to 6a or 1 to 6b of *EML4* were also designated variants 3a and 3b, respectively.

[6] Patent information: Garcia-Echeverria C, Kanazawa T, Kawahara E, Masuya K, Matsuura N, Miyake T, et al., inventors; Novartis AG, Novartis Pharma GmbH, IRM LLC, applicants. 2,4-Pyrimidinediamines useful in the treatment of neoplastic disease, inflammatory and immune system disorders. PCT WO 2005016894. 2005 Feb 24.

To isolate a full-length cDNA for EML4-ALK variant 3, we performed RT-PCR with total cDNA of a positive specimen (ID no. 2075) and with a sense strand primer targeted to the 5′ untranslated region (UTR) of *EML4* mRNA and an antisense strand primer targeted to the 3′ UTR of *ALK* mRNA. One-step PCR analysis yielded cDNA products for both *EML4-ALK* variants 3a and 3b (Fig. 1*C*; Supplementary Fig. S1).

The EML4 protein contains an amino-terminal basic domain followed by a hydrophobic echinoderm microtubule–associated protein–like protein (HELP) domain and WD repeats (14). Given that exons 1 to 6 of *EML4* encode the basic domain, the proteins encoded by the variant 3 cDNAs contain the entire basic domain of EML4 directly linked to the catalytic domain of ALK (Fig. 1*D*). The fact that the basic domain was found to be essential for both the self-dimerization and oncogenic activity of EML4-ALK (5) suggested that the variant 3 isoforms likely also possess transforming activity.

Chromosome rearrangement responsible for generation of *EML4-ALK* variant 3. To show the presence of a chromosome rearrangement responsible for the generation of *EML4-ALK* variant

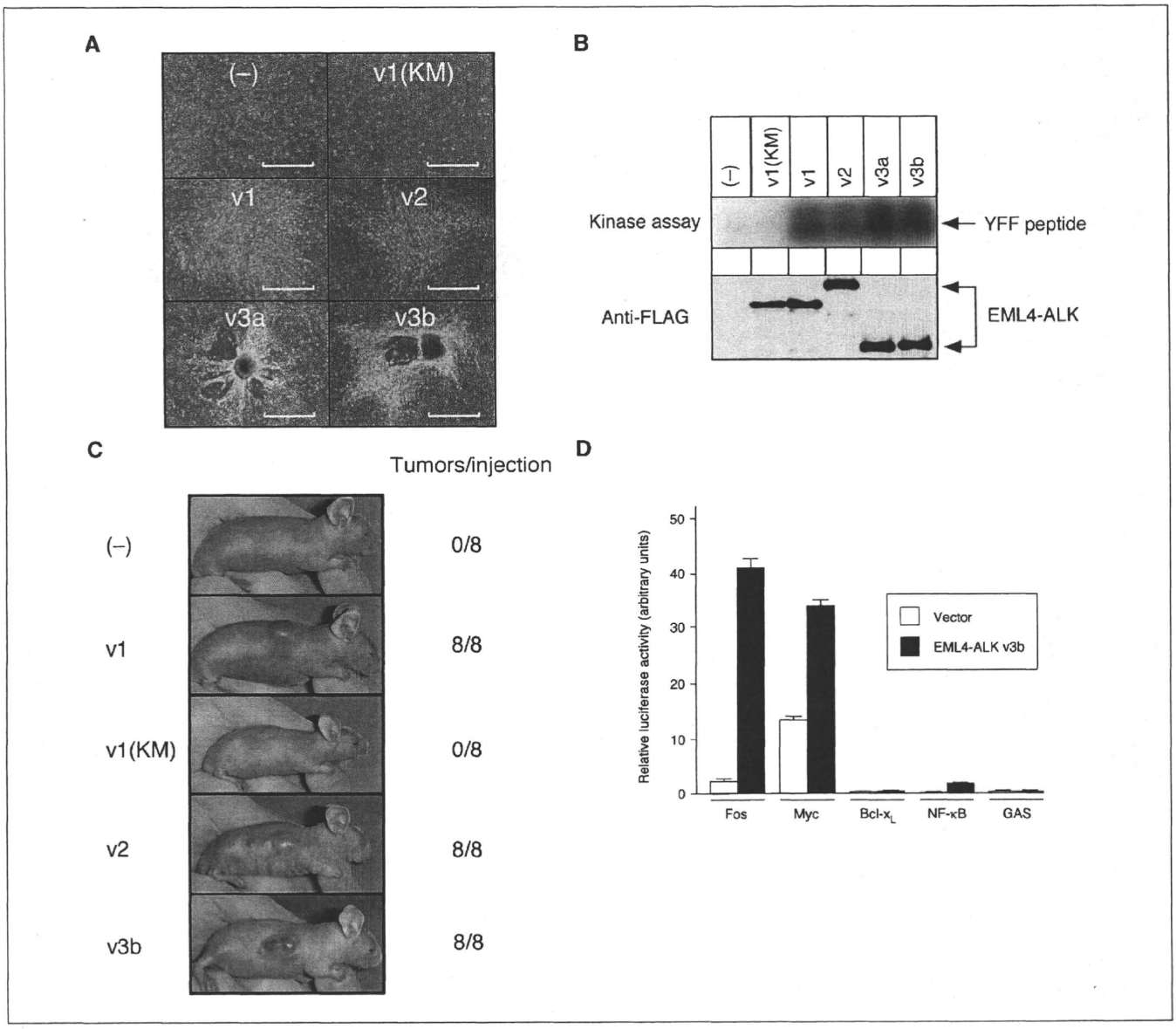

Figure 3. Transforming potential of EML4-ALK variants. *A*, focus formation assay. Mouse 3T3 fibroblasts were transfected with the empty expression plasmid [(–)] or with plasmids for wild-type (*v1*) or K589M mutant [*v1(KM)*] forms of variant 1, variant 2 (*v2*), variant 3a (*v3a*), or variant 3b (*v3b*) of FLAG-tagged EML4-ALK. The cells were photographed after culture for 18 d. *Bar*, 1 mm. *B, in vitro* kinase assay. HEK293 cells expressing the various FLAG-tagged variants of EML4-ALK were lysed and subjected to immunoprecipitation with antibodies to FLAG, and the resulting precipitates were assayed for kinase activity with the synthetic YFF peptide (*top*) or subjected to immunoblot analysis with antibodies to FLAG (*bottom*). *C, in vivo* assay of tumorigenicity. 3T3 cells expressing the indicated EML4-ALK variants were injected s.c. into nu/nu mice, and tumor formation was examined after 20 d. The number of tumors formed per eight injections is indicated on the right. *D*, analysis of EML4-ALK signaling with luciferase-based reporter plasmids. HEK293 cells were transfected with an expression plasmid for EML4-ALK variant 3b (or with the empty vector) together with reporter plasmids containing the promoter fragment of *Fos*, *Myc*, or *Bcl-x$_L$* gene; the DNA binding sequence for NF-κB; or the GAS sequence. Cells were cultured for 2 d, lysed, and assayed for luciferase activity. The activity of firefly luciferase was normalized by that of *Renilla* luciferase. *Columns*, mean of three experiments; *bars*, SD.

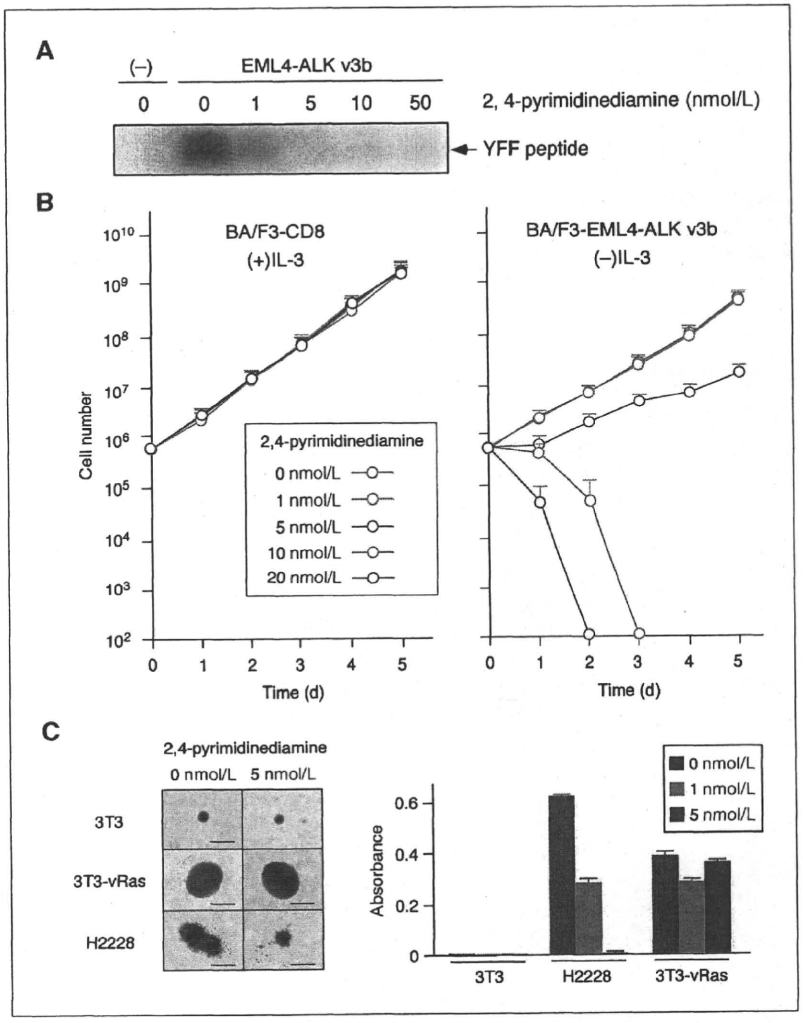

Figure 4. Essential role of EML4-ALK kinase activity in malignant transformation. *A*, lysates of HEK293 cells expressing FLAG-tagged EML4-ALK variant 3b (*v3b*) were divided into five equal portions, and each portion was subjected to immunoprecipitation with antibodies to FLAG. The immunoprecipitates were washed with kinase buffer [10 mmol/L HEPES-NaOH (pH 7.4), 50 mmol/L NaCl, 5 mmol/L $MgCl_2$, 5 mmol/L $MnCl_2$, 0.1 mmol/L Na_3VO_4] containing 0, 1, 5, 10, or 50 nmol/L of 2,4-pyrimidinediamine and then incubated for 30 min at room temperature for assay of kinase activity with the YFF peptide in the continued absence or presence of 2,4-pyrimidinediamine. The same amount of lysate of cells transfected with the empty vector was also subjected to immunoprecipitation and assayed as a negative control (–). *B*, mouse BA/F3 cells expressing CD8 alone were cultured in the presence of IL-3 (1 ng/mL) and the indicated concentrations of 2,4-pyrimidinediamine (*left*). BA/F3 cells expressing both CD8 and EML4-ALK variant 3b were cultured with the indicated concentrations of 2,4-pyrimidinediamine but without IL-3 (*right*). Cell number was counted at the indicated times. *Points*, mean of three separate experiments; *bars*, SD. *C*, mouse 3T3 fibroblasts expressing (or not) v-Ras or NCI-H2228 cells were cultured in a spheroid culture plate for 2 d, after which 2,4-pyrimidinediamine was added to the culture medium at a concentration of 0, 1, or 5 nmol/L. The cells were photographed after culture for an additional 5 d (*left*). *Bar*, 4 mm. Cell number in each well was also assessed at the same time with the use of the WST-1 assay (*right*). *Columns*, mean of three wells from a representative experiment; *bars*, SD.

3, we attempted to amplify the fusion point between the two genes from the genome of positive NSCLC cells. PCR with primers targeted to regions flanking the putative fusion point yielded a product of ~8 kbp with the genomic DNA of tumor ID no. 7969 (data not shown). Our failure to detect an unambiguous PCR product with genomic DNA of tumor ID no. 2075 may indicate that the breakpoint in intron 6 of *EML4* in this specimen is too distant from exon 6 to be readily amplified by PCR (intron 6 of *EML4* is >16 kbp). Nucleotide sequencing of the PCR product for tumor ID no. 7969 revealed that intron 6 of *EML4* was disrupted at a position ~7.1 kbp downstream of exon 6b and was joined to a point 749 bp upstream of exon 20 of *ALK* (Fig. 2*A*).

We also confirmed the chromosome rearrangement involving *EML4* and *ALK* by FISH analysis of cells from tumor ID no. 7969 (Fig. 2*B*) and tumor ID no. 2075 (data not shown) with differentially labeled probes for the two genes. Both genes map to the short arm of chromosome 2 within a distance of ~12 Mbp. The tumor cells exhibited fusion signals (corresponding to *EML4-ALK*) in addition to a pair of isolated green and red signals (corresponding to the two genes on the normal chromosome 2). The chromosome rearrangement involving the *ALK* locus was further verified with a different set of fluorescent probes (Supplementary Fig. S2).

Transforming activity of EML4-ALK variant 3. To compare the transforming potential of variants 1, 2, 3a, and 3b of EML4-ALK, we introduced expression plasmids for each variant into mouse 3T3 fibroblasts for assay of focus formation. No transformed foci were detected for cells transfected with the empty plasmid or with a plasmid for a kinase-inactive mutant (K589M) of EML4-ALK variant 1 (5) in which Lys^{589} in the ATP binding site of the catalytic domain is replaced with Met (Fig. 3*A*). In contrast, variants 3a and 3b of EML4-ALK each exhibited marked transforming activity that was not less than that of variant 1 or 2. To examine directly the tyrosine kinase activity of EML4-ALK variants, we subjected HEK293 cells expressing each of these variants to an *in vitro* kinase assay with a synthetic YFF peptide (7). Again, both variants 3a and 3b exhibited marked kinase activity that was not less than that of variant 1 or 2 (Fig. 3*B*). Similarly, in a tumorigenicity assay with nude mice, 3T3 cells expressing EML4-ALK variant 3b formed large subcutaneous tumors at all injection sites (Fig. 3*C*). Consistent with our previous observations (5), cells expressing variant 1 or 2 of EML4-ALK also formed tumors.

To examine the intracellular signaling pathways activated by EML4-ALK, we linked the luciferase cDNA to the promoter fragment of *Fos*, *Myc*, or *Bcl-x_L* gene (10–12); the DNA binding sequence for NF-κB; or the GAS sequence [a target site of the transcription factors signal transducers and activators of transcription (STAT)-1 and STAT3; ref. 15]. The resulting constructs were then introduced into HEK293 cells together with an

expression plasmid for EML4-ALK variant 3b. EML4-ALK variant 3b markedly activated the promoters of the *Fos* and *Myc* genes (Fig. 3*D*), consistent with the transforming potential of EML4-ALK. In contrast, although STAT3 has been shown to be a downstream target of the NPM-ALK fusion protein (16), EML4-ALK did not activate the GAS sequence, suggesting that STAT3 is unlikely to be a major target of EML4-ALK, as was shown in an EML4-ALK–positive lung cancer cell line by a proteomics approach (17). The distinct subcellular localizations of the two ALK fusion proteins [EML4-ALK in the cytoplasm (5) and NPM-ALK in both the nucleus and cytoplasm (18)] may account for this difference. Whereas EML4-ALK did not activate the *Bcl-x_L* gene promoter, it induced a small but significant increase in the activity of the NF-κB binding sequence ($P = 1.86 \times 10^{-4}$, Student's t test).

Several compounds have recently been identified as specific inhibitors of the kinase activity of ALK and as potential drugs for the treatment of lymphoma positive for *NPM-ALK* (19). We examined the effects of one such inhibitor, 2,4-pyrimidinediamine, on the transforming potential of EML4-ALK. We first determined the effect of this inhibitor on the kinase activity of EML4-ALK variant 3b immunoprecipitated from transfected cells. 2,4-Pyrimidinediamine inhibited the kinase activity of EML4-ALK in a concentration-dependent manner, with a concentration of 1 nmol/L reducing the kinase activity to <50% of the control value (Fig. 4*A*).

We also introduced EML4-ALK variant 3b and CD8 (or CD8 alone) into the IL-3–dependent hematopoietic cell line BA/F3 (9) and then purified the resulting CD8-positive cell populations. 2,4-Pyrimidinediamine, even at a concentration of 20 nmol/L, did not affect the IL-3–dependent growth of BA/F3 cells expressing only CD8 (Fig. 4*B*), indicating that this agent does not inhibit mitogenic signaling mediated by Janus kinase in BA/F3 cells. Expression of EML4-ALK rendered BA/F3 cells independent of IL-3 for growth, but the cells expressing the fusion protein also rapidly underwent cell death on exposure to 2,4-pyrimidinediamine (Fig. 4*B*).

Finally, we examined the effect of 2,4-pyrimidinediamine on lung cancer cells that express endogenous EML4-ALK variant 3. The human lung cancer cell line NCI-H2228 expresses EML4-ALK variants 3a and 3b (data not shown) and forms spheroids in a three-dimensional spheroid culture system (Fig. 4*C*; ref. 20). Whereas 3T3 fibroblasts are unable to form such spheroids, expression of v-Ras in these cells results in the formation of large spheroids in culture. Whereas 2,4-pyrimidinediamine did not affect the proliferation of 3T3 cells expressing v-Ras in this system, it inhibited the growth of NCI-H2228 cells in a concentration-dependent manner (Fig. 4*C*). These data thus indicate that EML4-ALK is essential for the growth of cancer cells expressing this oncokinase.

In conclusion, we have identified novel isoforms of *EML4-ALK* in two patients with NSCLC. A chromosome inversion within 2p was shown to connect intron 6 of *EML4* to intron 19 of *ALK* and to be responsible for the generation of fusion cDNAs connecting exons 1 to 6a or exons 1 to 6b of *EML4* to exon 20 of *ALK*. Given that fusion cDNAs with or without exon 6b of *EML4* were each present in the two patients, EML4-ALK variant 3a and 3b proteins are likely to be coexpressed in NSCLC cells. Although RT-PCR analysis to detect *EML4-ALK* may provide a highly sensitive means to detect lung cancer, it is important that all variant forms of the fusion gene be assayed with appropriately designed primer sets. Given that all the identified variants possess prominent transforming activity, the newly revealed increased incidence of *EML4-ALK* fusion in NSCLC further increases the importance of the fusion gene as a therapeutic target for this intractable disorder.

Disclosure of Potential Conflicts of Interest

K. Takeuchi: Consultant, DAKO. The other authors disclosed no potential conflicts of interest.

Acknowledgments

Received 11/8/2007; revised 3/3/2008; accepted 4/22/2008.

Grant support: Grants-in-Aid for Scientific Research from the Ministry of Education, Culture, Sports, Science, and Technology of Japan; the Japan Society for the Promotion of Science; and grants from the Ministry of Health, Labor, and Welfare of Japan, the Smoking Research Foundation of Japan, the National Institute of Biomedical Innovation of Japan, and the Vehicle Racing Commemorative Foundation of Japan.

The costs of publication of this article were defrayed in part by the payment of page charges. This article must therefore be hereby marked *advertisement* in accordance with 18 U.S.C. Section 1734 solely to indicate this fact.

We thank Takashi Aoki and Yasunobu Sugiyama for technical assistance.

References

1. Jemal A, Siegel R, Ward E, et al. Cancer statistics, 2006. CA Cancer J Clin 2006;56:106–30.
2. Lynch TJ, Bell DW, Sordella R, et al. Activating mutations in the epidermal growth factor receptor underlying responsiveness of non-small-cell lung cancer to gefitinib. N Engl J Med 2004;350:2129–39.
3. Paez JG, Janne PA, Lee JC, et al. EGFR mutations in lung cancer: correlation with clinical response to gefitinib therapy. Science 2004;304:1497–500.
4. Shigematsu H, Lin L, Takahashi T, et al. Clinical and biological features associated with epidermal growth factor receptor gene mutations in lung cancers. J Natl Cancer Inst 2005;97:339–46.
5. Soda M, Choi YL, Enomoto M, et al. Identification of the transforming EML4-ALK fusion gene in non-small-cell lung cancer. Nature 2007;448:561–6.
6. Onishi M, Kinoshita S, Morikawa Y, et al. Applications of retrovirus-mediated expression cloning. Exp Hematol 1996;24:324–9.
7. Donella-Deana A, Marin O, Cesaro L, et al. Unique substrate specificity of anaplastic lymphoma kinase (ALK): development of phosphoacceptor peptides for the assay of ALK activity. Biochemistry 2005;44:8533–42.
8. Yamashita Y, Kajigaya S, Yoshida K, et al. Sak serine/threonine kinase acts as an effector of Tec tyrosine kinase. J Biol Chem 2001;276:39012–20.
9. Palacious R, Steinmetz M. IL-3 dependent mouse clones that express B-220 surface antigen, contain Ig genes in germ-line configuration, and generate B lymphocytes *in vivo*. Cell 1985;41:727–34.
10. Hu Q, Milfay D, Williams LT. Binding of NCK to SOS and activation of ras-dependent gene expression. Mol Cell Biol 1995;15:1169–74.
11. Takeshita T, Arita T, Higuchi M, et al. STAM, signal transducing adaptor molecule, is associated with Janus kinase and involved in signaling for cell growth and c-myc induction. Immunity 1997;6:449–57.
12. Grillot DAM, Gonzalez-Garcia M, Ekhterae D, et al. Genomic organization, promoter region analysis, and chromosome localization of the mouse bcl-x gene. J Immunol 1997;158:4750–7.
13. Fujiwara S, Yamashita Y, Choi YL, et al. Transforming activity of purinergic receptor P2Y, G protein coupled, 8 revealed by retroviral expression screening. Leuk Lymphoma 2007;48:978–86.
14. Pollmann M, Parwaresch R, Adam-Klages S, Kruse ML, Buck F, Heidebrecht HJ. Human EML4, a novel member of the EMAP family, is essential for microtubule formation. Exp Cell Res 2006;312:3241–51.
15. Wesoly J, Szweykowska-Kulinska Z, Bluyssen HA. STAT activation and differential complex formation dictate selectivity of interferon responses. Acta Biochim Pol 2007;54:27–38.
16. Marzec M, Kasprzycka M, Ptasznik A, et al. Inhibition of ALK enzymatic activity in T-cell lymphoma cells induces apoptosis and suppresses proliferation and STAT3 phosphorylation independently of Jak3. Lab Invest 2005;85:1544–54.
17. Rikova K, Guo A, Zeng Q, et al. Global survey of phosphotyrosine signaling identifies oncogenic kinases in lung cancer. Cell 2007;131:1190–203.
18. Duyster J, Bai RY, Morris SW. Translocations involving anaplastic lymphoma kinase (ALK). Oncogene 2001;20:5623–37.
19. Galkin AV, Melnick JS, Kim S, et al. Identification of NVP-TAE684, a potent, selective, and efficacious inhibitor of NPM-ALK. Proc Natl Acad Sci U S A 2007;104:270–5.
20. Kunita A, Kashima TG, Morishita Y, et al. The platelet aggregation-inducing factor aggrus/podoplanin promotes pulmonary metastasis. Am J Pathol 2007;170:1337–47.

A mouse model for *EML4-ALK*-positive lung cancer

Manabu Soda[a,b], Shuji Takada[a], Kengo Takeuchi[c], Young Lim Choi[a], Munehiro Enomoto[a], Toshihide Ueno[a], Hidenori Haruta[a], Toru Hamada[a], Yoshihiro Yamashita[a], Yuichi Ishikawa[c], Yukihiko Sugiyama[b], and Hiroyuki Mano[a,d,1]

Divisions of [a]Functional Genomics and [b]Pulmonary Medicine, Jichi Medical University, Tochigi 329-0498, Japan; [c]Division of Pathology, The Cancer Institute, Japanese Foundation for Cancer Research, Tokyo 135-8550, Japan; and [d]Core Research for Evolutional Science and Technology, Japan Science and Technology Agency, Saitama 332-0012, Japan

Edited by John D. Minna, University of Texas Southwestern Medical Center, Dallas, TX, and accepted by the Editorial Board October 17, 2008 (received for review June 2, 2008)

EML4-ALK is a fusion-type protein tyrosine kinase that is generated in human non-small-cell lung cancer (NSCLC) as a result of a recurrent chromosome inversion, inv (2)(p21p23). Although mouse 3T3 fibroblasts expressing human EML4-ALK form transformed foci in culture and s.c. tumors in nude mice, it has remained unclear whether this fusion protein plays an essential role in the carcinogenesis of NSCLC. To address this issue, we have now established transgenic mouse lines that express EML4-ALK specifically in lung alveolar epithelial cells. All of the transgenic mice examined developed hundreds of adenocarcinoma nodules in both lungs within a few weeks after birth, confirming the potent oncogenic activity of the fusion kinase. Although such tumors underwent progressive enlargement in control animals, oral administration of a small-molecule inhibitor of the kinase activity of ALK resulted in their rapid disappearance. Similarly, whereas i.v. injection of 3T3 cells expressing EML4-ALK induced lethal respiratory failure in recipient nude mice, administration of the ALK inhibitor effectively cleared the tumor burden and improved the survival of such animals. These data together reinforce the pivotal role of EML4-ALK in the pathogenesis of NSCLC in humans, and they provide experimental support for the treatment of this intractable cancer with ALK inhibitors.

transgenic mouse | surfactant protein C | molecular targeted therapy

Lung cancer remains the leading cause of cancer deaths, with almost 1.3 million people dying annually from this condition worldwide (www.who.int/cancer/en). Although a variety of chemotherapeutic regimens have been developed to treat this intractable disease, their efficacy is limited and depends on cancer subtype. Non-small-cell lung cancer (NSCLC) accounts for 80–85% of all lung cancer cases and is less sensitive to cytotoxic drugs than is small cell lung cancer. Unless tumor cells are surgically resected at an early clinical stage, individuals with NSCLC can expect a median survival time of less than 1 year (1).

A subset of individuals with NSCLC (mostly nonsmokers, young females, and those of Asian ethnicity) have been shown to harbor mutations in the epidermal growth factor receptor (EGFR) gene (2–4). Such mutations result in constitutive activation of the EGFR tyrosine kinase, the oncogenic potential of which has been demonstrated in a transgenic mouse system (5). Small-molecule drugs that specifically inhibit the catalytic activity of EGFR have been found to exhibit clinical efficacy in the treatment of NSCLC patients, especially in those with an activated EGFR (6, 7).

We recently developed a system for the construction of retroviral cDNA libraries from small quantities of clinical specimens (8–10), and we applied this technology to NSCLC to screen for oncogenes that might be potential drug targets (11). With the use of a focus-formation assay performed with mouse 3T3 fibroblasts, we identified a fusion-type oncogene, *EML4-ALK*, in an NSCLC specimen of a smoker (12). A small inversion within the short arm of chromosome 2 was found to result in the ligation of *EML4* and *ALK*, leading to the production of a fusion protein consisting of the amino-terminal portion of EML4 and the intracellular region of the protein tyrosine kinase ALK. The coiled-coil domain within this portion of EML4 mediates the constitutive dimerization and activation of EML4-ALK, which is responsible for the generation of transformed cell foci in culture and the formation by these cells of s.c. tumors in nude mice. Although the inv (2)(p21p23) rearrangement responsible for the fusion event occurs recurrently in NSCLC patients, it remains to be demonstrated that *EML4-ALK* plays an essential role in the carcinogenesis of NSCLC harboring the fusion gene.

To address this issue, we have now engineered the expression of *EML4-ALK* in lung epithelial cells of transgenic mice. The surfactant protein C gene (*SPC*) is specifically expressed in type 2 alveolar epithelial cells, and a fragment of its promoter has been used widely for establishment of mouse lines that express transgenes specifically in lung epithelial cells (13–15). We therefore generated independent mouse lines in which *EML4-ALK* expression is driven by the *SPC* promoter, and we found that all such mice develop hundreds of adenocarcinoma nodules in both lungs within only a few weeks after birth. Furthermore, inhibition of EML4-ALK activity with a small-molecule drug induced rapid death of the tumor cells.

Results

Generation of *EML4-ALK* Transgenic Mice. To generate mice with lung-specific expression of *EML4-ALK*, we ligated a fragment of the *SPC* promoter (≈3.7 kbp) to a cDNA for EML4-ALK variant 1 with an amino-terminal FLAG epitope tag (12). The cDNA was, in turn, attached to an RNA splicing cassette and a polyadenylation signal (Fig. 1*A*). The transgene construct (≈8.3 kbp) was then injected into pronuclear-stage embryos of C57BL/6J mice, and the resulting progeny were screened for the presence of the transgene by Southern blot analysis. Seven founder mice positive for incorporation of the transgene (copy number per diploid genome ranging from 1 to 30) were obtained (Fig. 1*B* and data not shown). Two transgenic lines (501-3 and 502-4, with 10 and 30 copies of the transgene per genome, respectively) were independently maintained by backcrossing to C57BL/6J mice. To confirm the lung-specific expression of the transgene, we performed RT-PCR analysis to detect *EML4-ALK* mRNA in an F_1 mouse of the 502-4 line. The transgene was expressed in lung tissue (containing adenocarcinoma nodules, see below) but not in liver, esophagus, stomach, colon, brain, kidney, or uterus (Fig. 1*C*).

Detection of Multiple Lung Adenocarcinoma Nodules in the Transgenic Mice. One founder mouse (503-6, with 3 copies of the transgene per genome) (Fig. 1*B*) died 3 weeks after birth. Postmortem

Author contributions: Y.I., Y.S., and H.M. designed research; M.S., S.T., K.T., Y.L.C., M.E., T.U., H.H., T.H., Y.Y., and Y.I. performed research; and H.M. wrote the paper.

Conflict of interest statement: K.T. is a consultant for Dako.

This article is a PNAS Direct Submission. J.D.M. is a guest editor invited by the Editorial Board.

[1]To whom correspondence should be addressed. E-mail: hmano@jichi.ac.jp.

This article contains supporting information online at www.pnas.org/cgi/content/full/0805381105/DCSupplemental.

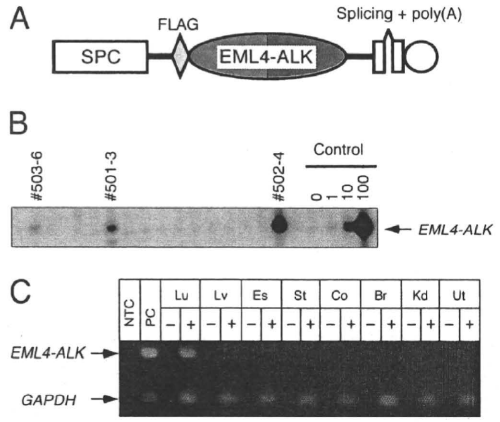

Fig. 1. Generation of transgenic mouse lines for *EML4-ALK*. (*A*) A cDNA for FLAG-tagged EML4-ALK was inserted between the *SPC* promoter and both splicing and polyadenylation [poly(A)] signal sequences. (*B*) Genomic DNA was isolated from the tail of founder mice generated from pronuclear-stage C57BL/6J embryos and was subjected to Southern blot analysis with full-length *EML4-ALK* cDNA as a probe. Control samples on the right comprised mouse genomic DNA with 0, 1, 10, or 100 copies of the transgene per diploid genome. The ID numbers of founder mice positive for the transgene are shown at the top. (*C*) Oligo(dT)-primed cDNA was synthesized from total RNA isolated from lung (Lu), liver (Lv), esophagus (Es), stomach (St), colon (Co), brain (Br), kidney (Kd), and uterus (Ut) of an F_1 mouse of the 502-4 line, with the reaction being performed in the presence (+) or absence (−) of reverse transcriptase. The cDNA preparations were then subjected to PCR with primer sets for *EML4-ALK* or for *GAPDH*, and the PCR products were separated by agarose gel electrophoresis and stained with ethidium bromide. The positions of the PCR products are indicated on the left. RT-PCR was also performed for a no-template control (NTC) and for a human NSCLC specimen harboring *EML4-ALK* variant 1 as a positive control (PC).

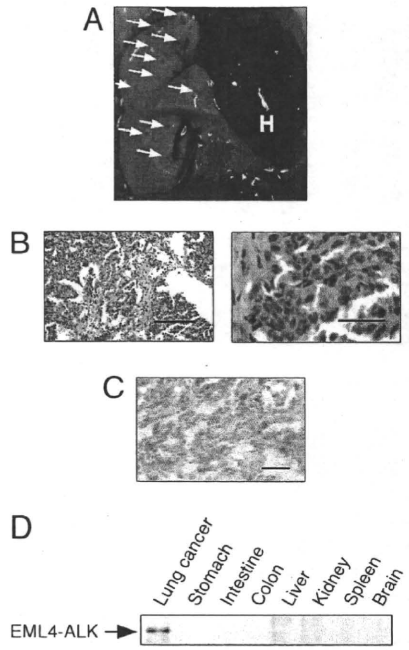

Fig. 2. Development of lung adenocarcinoma in *EML4-ALK* transgenic mice. (*A*) Hundreds of adenocarcinoma nodules (arrows) were apparent in the lungs of a founder mouse (503-6) that died 3 weeks after birth. H, heart. (*B*) Microscopic examination of the nodules shown in *A* after staining with H&E. Images at low (*Left*) and high (*Right*) magnification are shown with scale bars of 200 and 40 μm, respectively. Some tumors exhibited obvious scar formation, suggesting that they were invasive carcinomas. (*C*) Immunohistochemical analysis with antibodies to ALK of one of the nodules shown in *A* revealed a pattern of cytoplasmic staining with granular accentuations. (Scale bar, 50 μm.) (*D*) Immunoprecipitates prepared with antibodies to FLAG from the indicated tissues of an F_1 mouse of the 502-4 line were subjected to immunoblot analysis with the same antibodies. The position of EML4-ALK is shown at the left.

examination revealed hundreds of nodules in both lungs of this animal (Fig. 2*A*) and that these nodules were filled with adenocarcinoma cells (Fig. 2*B*). Immunohistochemical analysis with antibodies to ALK showed a diffuse cytoplasmic staining with granular accentuations in the neoplastic cells (Fig. 2*C*), consistent with the results of a similar analysis of *EML4-ALK*-positive human tumors (16). The level of immunoreactivity in the lungs of the transgenic mouse, however, was substantially lower than that in *EML4-ALK*-positive human specimens, suggestive of a lower level of expression for the EML4-ALK protein.

Detection of EML4-ALK by immunoblot analysis with antibodies to the FLAG tag confirmed a low-level but lung-specific expression of the kinase (Fig. 2*D*). Pathology and computed tomography (CT) examinations (see below) of the progeny of the maintained transgenic mouse lines (501-3 and 502-4) also revealed the development of multiple adenocarcinoma nodules in their lungs at only a few weeks after birth, demonstrating an essential role for the EML4-ALK kinase in NSCLC carcinogenesis. There was no discernable difference in tumor-forming activity between the 2 transgenic lines. We thus used both of these lines for further analyses.

Treatment of NSCLC-Positive Transgenic Mice with an ALK-Specific Inhibitor. To observe the development of NSCLC in the transgenic mice, we performed a series of CT scans of the chest. Multiple large nodules, some with infiltrative profiles of NSCLC, were detected in the lungs of progeny mice [Fig. 3*A*; also see supporting information (SI) Movie S1]. Other progeny with similar CT findings were subjected to pathology examination, confirming that such CT profiles reflected tumor expansion and infiltration in the lungs (data not shown). Examination of other organs of these mice failed to detect metastatic tumor nodules.

Several chemical compounds that specifically inhibit the tyrosine kinase activity of ALK have been identified (17–19). One such 2,4-pyrimidinediamine derivative has a median inhibitory concentration for ALK of <10 nM and a high specificity to ALK (Fig. S1) (20). We therefore examined whether peroral treatment with this compound (10 mg per kg of body weight per day) might inhibit the growth or induce the death of the adenocarcinoma cells in the transgenic mice. CT scans were performed after 0, 11, and 25 days of treatment for all 10 mice in each of the treatment and control (vehicle) groups, and a sequential examination of CT profiles was undertaken for each animal. The tumor mass developed rapidly in both lungs for most of the animals in the control group (Fig. 3*A*; also see Movie S2). Multiple nodules of various sizes newly appeared in the lungs, and the existing nodules became enlarged. In contrast, treatment with the ALK inhibitor greatly reduced the tumor burden in all mice (Fig. 3*B*). A large tumor in the lower lobe of the right lung in mouse 373, for instance, was reduced to ≈30% of its original size (based on the cross-section at the chest level in Fig. 3*B*) after only 11 days of the drug treatment and was almost undetectable by CT after treatment for 25 days (Movie S3). Sequential CT examination of another mouse (381) confirmed the pronounced activity of the ALK inhibitor (Fig. 3*B*; also see Movie S4 and Movie S5).

Mice in both groups were killed for pathology analysis after drug or vehicle administration for 2 months. Although multiple large tumor nodules were readily identified in the lungs of control mice, such nodules were apparent only occasionally in the treated animals (Fig. 3*C*), confirming the marked therapeutic effect of the ALK inhibitor. However, several small nodules were detected in the

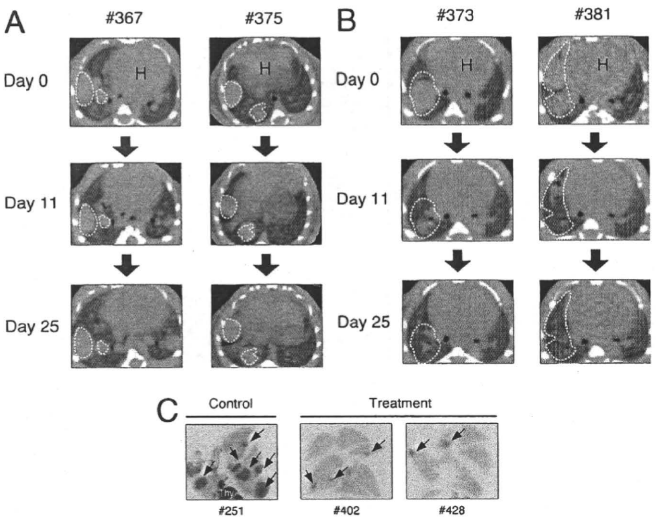

Fig. 3. Treatment of *EML4-ALK* transgenic mice with a specific ALK inhibitor. (*A* and *B*) Transgenic mice were subjected to daily peroral administration of vehicle (*A*) or ALK inhibitor (*B*) beginning at 4 weeks of age and were examined by CT scanning of the chest on days 0, 11, and 25. The ID numbers of the mice are shown at the top. H, heart. Tumors (indicated by broken lines) in both lungs underwent progressive enlargement in all control mice but became progressively smaller in all treated animals. (*C*) Macroscopic examination of the lungs from mice of the control and treatment groups at 2 months after the onset of treatment. The tissue was stained with H&E. The ID numbers of the mice are shown at the bottom. Cancer nodules are indicated by arrows. Thy, thymus.

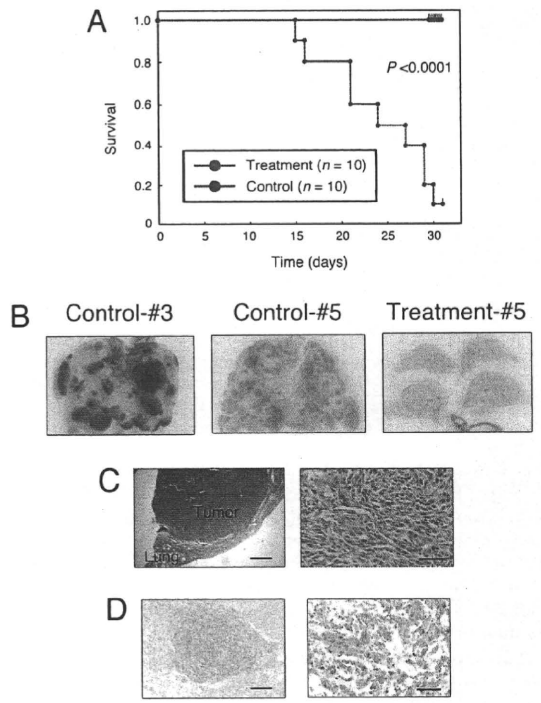

Fig. 4. Treatment with the ALK inhibitor of mice injected with EML4-ALK/3T3 cells. (*A*) Nude mice were injected i.v. with 2×10^5 3T3 cells expressing EML4-ALK variant 1 and were then immediately subjected to daily peroral administration of vehicle (control, $n = 10$) or ALK inhibitor (treatment, $n = 10$). Survival of the 2 cohorts is shown as a Kaplan–Meier plot and was compared by the log-rank test, with the calculated P value indicated. (*B*) Macroscopic examination of lungs isolated from mice of the control group at death or of the treatment group after treatment for 31 days. The tissue was stained with H&E. Most of the lungs in both control animals were occupied with transformed EML4-ALK/3T3 cells, whereas such cells were rarely observed in the treated animal. (*C*) Microscopic examination of lung tissue from a mouse of the control group after H&E staining. Images of low (*Left*) and high (*Right*) magnification are shown with scale bars of 500 and 50 μm, respectively. (*D*) Immunohistochemical analysis with antibodies to ALK of the nodules of EML4-ALK/3T3 cells that formed in the lungs of a mouse in the control group. Images of low (*Left*) and high (*Right*) magnification are shown with scale bars of 200 and 50 μm, respectively.

treated mice. Microscopic examination of the lungs of control and treated mice confirmed the changes observed by CT scanning and macroscopic analysis (data not shown). Even at this time point, we did not detect metastatic nodules in organs other than the lungs in either control or treated mice, and all animals in these cohorts survived the observation period.

Treatment of Mice Injected with 3T3 Cells Expressing EML4-ALK. Given that transgenic mice with lung cancer did not die by 6 months of age (with the exception of the one shown in Fig. 2*A* and another that died at 6 months after birth), we were not able to examine statistically the possible effect of the ALK inhibitor on survival in these animals. We therefore adopted another approach—that of loading mice with a large number of EML4-ALK-positive cells. We previously showed that mouse 3T3 fibroblasts expressing EML4-ALK (EML4-ALK/3T3) undergo transformation and generate s.c. tumors when injected into *nu/nu* mice (12). Such EML4-ALK/3T3 cells (2×10^5) were therefore injected i.v. into *nu/nu* mice ($n = 20$), and the ALK inhibitor was administered to half of these animals.

A total of 9 of the 10 untreated mice died within 1 month of injection with the EML4-ALK/3T3 cells (Fig. 4*A*). Postmortem examination of these mice revealed extensive dissemination of EML4-ALK-positive cells into the lungs (>60% of lung tissue was occupied with the transformed EML4-ALK/3T3 cells in all mice) (Fig. 4*B*). Pathology examination of the lungs revealed many nodules of various sizes that were filled with the EML4-ALK/3T3 fibroblasts (Fig. 4*C*). In a separate experiment, we confirmed that injection of parental 3T3 cells did not induce the formation of such nodules in the lungs or affect the survival of mice (data not shown).

To verify that the injected EML4-ALK/3T3 cells continued to express EML4-ALK, we stained tissue sections of the lungs of control mice with antibodies to ALK. All cells within nodules reacted with the antibodies (Fig. 4*D*), giving rise to a diffuse pattern of cytoplasmic staining with granular accentuations. Although the staining profile was similar to that observed for the transgenic mice, the staining intensity in the EML4-ALK/3T3 cell-injected animals was greater than that in the transgenic animals.

Similar to the results obtained with transgenic mice, transformed EML4-ALK/3T3 cells were not detected in any organs other than the lungs of the injected mice, with the exception of 2 animals in the control group (nos. 3 and 7). Given the massive infiltration of EML4-ALK/3T3 cells in the lungs of all mice in the control cohort, these mice likely died from respiratory failure. In the control no. 7 mouse, we detected pronounced infiltration of EML4-ALK/3T3 cells into both the mediastinum (Fig. S2*A*) and the diaphragm (Fig. S2*B*). Given that both of these structures are adjacent to the lungs and that this mouse had an exceptionally high tumor burden in the lungs (>90% of the lungs were occupied with EML4-ALK/3T3 cells; Fig. S2*C*), the presence of EML4-ALK/3T3 cells in the mediastinum and diaphragm was likely the result of direct invasion from the lungs rather than of distant metastasis.

Peroral administration of the ALK inhibitor markedly improved the outcome of mice injected with the transformed EML4-ALK/3T3 cells, with all 10 animals in the treatment group surviving the 1-month observation period ($P < 0.0001$, log-rank test) (Fig. 4*A*). The treated mice also were subjected to pathology analysis after this period, revealing the absence of EML4-

ALK/3T3 nodules from the lungs (Fig. 4*B*) and again demonstrating the high efficacy of the ALK inhibitor.

Discussion

We have shown here that the EML4-ALK fusion kinase plays an essential role in lung tumorigenesis. Hundreds of adenocarcinoma nodules developed simultaneously within a few weeks after birth in all independent lines of *EML4-ALK* transgenic mice examined. Given that the promoter fragment of *SPC* becomes active only at a late stage of gestation (21), a short period of *EML4-ALK* expression appears to be sufficient for full transformation. Although we did not examine *TP53* and *RB1* for possible abnormalities in the adenocarcinoma nodules of the transgenic mice, with both of these genes being frequently inactivated in human lung cancers (22), it is likely that only one (or at most a few) additional genetic event is required to generate cancer in EML4-ALK-expressing alveolar epithelial cells.

The expression level of EML4-ALK protein in the adenocarcinoma nodules of the transgenic mice was low. Given that the abundance of *EML4-ALK* mRNA in these nodules was found to be greater than that in human *EML4-ALK*-positive NSCLC specimens (data not shown), the expression of EML4-ALK protein appears to be suppressed in the mouse lung epithelial cells, possibly through translational or posttranslational mechanisms. The development of adenocarcinoma even at this low level of protein expression further reinforces the transforming activity of EML4-ALK.

Given the rapid development of NSCLC induced by EML4-ALK, the tumor cells are likely dependent for growth on the tyrosine kinase activity of the fusion protein. Such "oncogene addiction" (23) provides a potential target for the development of treatment strategies. We therefore tested whether inhibition of the enzymatic activity of EML4-ALK might reduce the tumor burden in the transgenic mice. The ALK inhibitor examined proved to be a promising candidate for the treatment of EML4-ALK-positive tumors. Furthermore, given the high sensitivity of the tumors in the transgenic mice to the ALK inhibitor, these animals provide a model system with which to examine the in vivo activity of other compounds or reagents targeted to ALK.

Many of the large tumors in the lungs of the transgenic mice changed to bullae or cysts after treatment with the ALK inhibitor, as revealed both by CT scanning (Fig. S3*A* and Movie S3 and Movie S5) and by pathology examination (Fig. S3*B*). Such a change was not described for treatment of activated EGFR-positive NSCLC in mouse models or humans with EGFR inhibitors (5, 6). A rapid induction of cell death by the ALK inhibitor in the transgenic mice may have triggered a collapse of the tumor burden within each nodule, thereby giving rise to bullae or cysts. Indeed, pathology examination revealed that a large tumor in 1 transgenic mouse (no. 250) became filled with necrotic tissue after treatment (Fig. S3*C*). However, the bullae cysts and necrotic tissue were still surrounded by remaining cancer cells (Fig. S3 *B* and *C*). Similarly, the lining tissue of some bullae cysts in the treated mice appeared to have a high density in CT scans (Fig. S3*A*), suggesting that peripheral cancer cells may survive in the nodules. Furthermore, small foci of cancer cells could be identified in the lungs of transgenic mice in the treatment cohort (Fig. 3*C*). Together, these various observations indicate that the current treatment protocol with the ALK inhibitor did not entirely eliminate tumor cells from the transgenic mice. Indeed, in a separate experiment transgenic mice treated with the 2,4-pyrimidinediamine for 25 days were examined 3 months after cessation of drug administration. Tumors of various sizes regrew in these mice (Fig. S4), indicative of the presence of surviving EML4-ALK-positive cancer cells in the animals after 25 days of drug treatment. Given that we have not tried other protocols or compounds, it remains unknown whether a total cure might be achieved by treatment for a longer period or with a higher dose of the same inhibitor or with a more potent compound. It is also possible that inhibition of additional signaling pathways, such as those mediated by phosphoinositide 3-kinase, mammalian target of rapamycin, or other protein tyrosine kinases (5, 24), may be required for a complete cure.

Despite the rapid growth of multiple tumors in the lungs of the transgenic mice, we failed to detect distant metastasis of such cancer cells in animals killed for analysis or in those that died within the total observation period of 6 months. However, we conclude that the tumors that developed in these mice had malignant characteristics on the basis of the following observations: (*i*) Histological analysis indicated that most tumors were noninvasive papillary adenocarcinomas, with some of them further showing obvious fibrosis and destruction of alveolar structures (Fig. 2*B*), a marker of invasion in human lung adenocarcinoma. (*ii*) Subcutaneous transplantation of tumor nodules that developed in the transgenic mice into the shoulder of *nu/nu* mice resulted in the growth of tumors at 6 of 8 injection sites in the recipient animals (Fig. S5*A*). (*iii*) Tumors that developed in the transgenic mice were shown to keep growing for at least 62 days in in vitro culture (Fig. S5*B*).

It is likely that expression of EML4-ALK (and probably other accompanying genetic changes) alone is not sufficient to render the cancer cells metastatic. It remains to be determined whether additional abnormalities in other oncogenes or tumor suppressor genes, such as *KRAS* or *LKB1* (25, 26), may lead to the generation of metastatic tumors in *EML4-ALK* transgenic mice.

Our present results have reinforced the importance of *EML4-ALK* in the pathogenesis of NSCLC in humans and have provided experimental support for the treatment of such intractable tumors with ALK inhibitors. Given that variants of *EML4-ALK* other than the variants 1 and 2 described in our original study (12) are now being identified (20, 27–29), it will be important to characterize all possible isoforms of *EML4-ALK* in humans to identify precisely the subgroup of patients who are candidates for future treatment with ALK inhibitors. Further to this goal, it will also be important to clarify the genetic changes that accompany the *EML4-ALK* fusion event as well as the downstream targets of EML4-ALK action in human NSCLC.

Materials and Methods

Generation of Transgenic Mice. A cDNA fragment encoding FLAG epitope-tagged EML4-ALK variant 1 (12) was ligated to the *SPC* promoter as well as to splicing and polyadenylation signals (Fig. 1*A*). The expression cassette was injected into pronuclear-stage embryos of C57BL/6J mice (PhoenixBio), and the copy number of the transgene was examined by Southern blot analysis with DNA from the tail of founder animals. All animal procedures were performed with the approval of the scientific committee for animal experiments of Jichi Medical University.

For detection of mRNAs derived from *EML4-ALK* and the glyceraldehyde-3-phosphate dehydrogenase gene (*GAPDH*), total RNA was isolated from the organs of transgenic mice with the use of an RNeasy Mini kit (Qiagen) and was subjected to reverse transcription with SuperScript III reverse transcriptase (Invitrogen) and an oligo(dT) primer. Both reverse transcription and subsequent PCR analysis for each gene were performed as described previously (12).

For analysis of EML4-ALK protein in mice, organ homogenates were prepared with an Nonidet P-40 lysis buffer and subjected to immunoprecipitation with mouse monoclonal antibodies to FLAG (Millipore). The resulting precipitates were then subjected to immunoblot analysis with the same antibodies and a SuperSignal chemiluminescence kit (Pierce Biotechnology).

Pathology Examination. For immunohistochemical staining of EML4-ALK in EML4-ALK/3T3 cells, paraffin-embedded sections were depleted of paraffin with xylene, rehydrated with a graded series of ethanol solutions, and stained with mouse monoclonal antibodies to ALK (ALK1; Dako) at a dilution of 1:20 and with an EnVision+DAB system (Dako). The sections were subjected to heat-induced antigen retrieval with Target Retrieval Solution, pH 9.0 (Dako), before exposure to the antibodies. For detection of EML4-ALK in transgenic mice, cryostat sections were fixed with 4% paraformaldehyde in 0.1 M sodium phosphate buffer (pH 7.4) for 10 min, treated with Target Retrieval Solution, pH 9.0, and immunostained with the monoclonal antibodies to ALK and the EnVision+DAB system.

Treatment with ALK Inhibitor. For the experiments based on i.v. administration of EML4-ALK/3T3 cells, the cells (2×10^5) were injected into the tail vein of 4-week-old *nu/nu* mice (Clea Japan). An inhibitor specific for the tyrosine kinase activity of ALK [example 3-39 in the patent application: Garcia-Echeverria C, *et al.*, inventors; Novartis AG, Novartis Pharma GmbH, IRM LLC, applicants (24 Feb 2005). 2,4-Pyrimidinediamines useful in the treatment of neoplastic disease and in inflammatory and immune system disorders. PCT WO 2005016894] was synthesized by Astellas Pharma and was orally administered each day at a dose of 10 mg/kg to the injected mice or to *EML4-ALK*-transgenic mice. Sequential examination of lung tumors was performed with an X-ray CT apparatus for experimental animals (LCT-100; Aloka).

ACKNOWLEDGMENTS. We thank Koichi Hagiwara (Saitama Medical University, Saitama, Japan) for kindly providing the human *SPC* promoter fragment as well as Keiko Shiozawa and Tomoyo Kakita for technical assistance. This study was supported in part by a grant for Research on Human Genome Tailor-made from the Ministry of Health, Labor, and Welfare of Japan; by Grants-in-Aid for Scientific Research on Priority Areas from the Ministry of Education, Culture, Sports, Science, and Technology of Japan; and by grants from the Japan Society for the Promotion of Science, the National Institute of Biomedical Innovation, the Princess Takamatsu Cancer Research Fund, the Takeda Science Foundation, the Uehara Memorial Foundation, the Smoking Research Foundation, the Vehicle Racing Commemorative Foundation, and the NOVARTIS Foundation (Japan) for the Promotion of Science.

1. Schiller JH, *et al.* (2002) Comparison of four chemotherapy regimens for advanced non-small-cell lung cancer. *N Engl J Med* 346:92–98.
2. Paez JG, *et al.* (2004) EGFR mutations in lung cancer: Correlation with clinical response to gefitinib therapy. *Science* 304:1497–1500.
3. Pao W, *et al.* (2004) EGF receptor gene mutations are common in lung cancers from "never smokers" and are associated with sensitivity of tumors to gefitinib and erlotinib. *Proc Natl Acad Sci USA* 101:13306–13311.
4. Shigematsu H, *et al.* (2005) Clinical and biological features associated with epidermal growth factor receptor gene mutations in lung cancers. *J Natl Cancer Inst* 97:339–346.
5. Li D, *et al.* (2007) Bronchial and peripheral murine lung carcinomas induced by T790M-L858R mutant EGFR respond to HKI-272 and rapamycin combination therapy. *Cancer Cell* 12:81–93.
6. Lynch TJ, *et al.* (2004) Activating mutations in the epidermal growth factor receptor underlying responsiveness of non-small-cell lung cancer to gefitinib. *N Engl J Med* 350:2129–2139.
7. Kris MG, *et al.* (2003) Efficacy of gefitinib, an inhibitor of the epidermal growth factor receptor tyrosine kinase, in symptomatic patients with non-small cell lung cancer: A randomized trial. *J Am Med Assoc* 290:2149–2158.
8. Hatanaka H, *et al.* (2007) Transforming activity of purinergic receptor P2Y, G-protein coupled, 2 revealed by retroviral expression screening. *Biochem Biophys Res Commun* 356:723–726.
9. Fujiwara S, *et al.* (2007) Transforming activity of purinergic receptor P2Y, G protein coupled, 8 revealed by retroviral expression screening. *Leuk Lymphoma* 48:978–986.
10. Choi YL, *et al.* (2007) Identification of a constitutively active mutant of JAK3 by retroviral expression screening. *Leuk Res* 31:203–209.
11. Besse B, Ropert S, Soria JC (2007) Targeted therapies in lung cancer. *Ann Oncol* 18(suppl 9):ix135–ix142.
12. Soda M, *et al.* (2007) Identification of the transforming *EML4-ALK* fusion gene in non-small-cell lung cancer. *Nature* 448:561–566.
13. Mishra A, Weaver TE, Beck DC, Rothenberg ME (2001) Interleukin-5-mediated allergic airway inflammation inhibits the human surfactant protein C promoter in transgenic mice. *J Biol Chem* 276:8453–8459.
14. Duan W, *et al.* (2002) Lung-specific expression of human mutant p53–273H is associated with a high frequency of lung adenocarcinoma in transgenic mice. *Oncogene* 21:7831–7838.
15. Zhao B, *et al.* (2000) Transgenic mouse models for lung cancer. *Exp Lung Res* 26:567–579.
16. Inamura K, *et al.* (2008) *EML4-ALK* fusion is linked to histological characteristics in a subset of lung cancers. *J Thorac Oncol* 3:13–17.
17. Chiarle R, Voena C, Ambrogio C, Piva R, Inghirami G (2008) The anaplastic lymphoma kinase in the pathogenesis of cancer. *Nat Rev Cancer* 8:11–23.
18. McDermott U, *et al.* (2007) Identification of genotype-correlated sensitivity to selective kinase inhibitors by using high-throughput tumor cell line profiling. *Proc Natl Acad Sci USA* 104:19936–19941.
19. Galkin AV, *et al.* (2007) Identification of NVP-TAE684, a potent, selective, and efficacious inhibitor of NPM-ALK. *Proc Natl Acad Sci USA* 104:270–275.
20. Choi YL, *et al.* (2008) Identification of novel isoforms of the EML4-ALK transforming gene in non-small cell lung cancer. *Cancer Res* 68:4971–4976.
21. Korfhagen TR, *et al.* (1990) Cis-acting sequences from a human surfactant protein gene confer pulmonary-specific gene expression in transgenic mice. *Proc Natl Acad Sci USA* 87:6122–6126.
22. Testa JR, *et al.* (1997) Advances in the analysis of chromosome alterations in human lung carcinomas. *Cancer Genet Cytogenet* 95:20–32.
23. Sharma SV, Settleman J (2007) Oncogene addiction: Setting the stage for molecularly targeted cancer therapy. *Genes Dev* 21:3214–3231.
24. Engelman JA, *et al.* (2007) MET amplification leads to gefitinib resistance in lung cancer by activating ERBB3 signaling. *Science* 316:1039–1043.
25. Ji H, *et al.* (2007) LKB1 modulates lung cancer differentiation and metastasis. *Nature* 448:807–810.
26. Huang CL, *et al.* (1998) Mutations of p53 and K-ras genes as prognostic factors for non-small cell lung cancer. *Int J Oncol* 12:553–563.
27. Rikova K, *et al.* (2007) Global survey of phosphotyrosine signaling identifies oncogenic kinases in lung cancer. *Cell* 131:1190–1203.
28. Koivunen JP, *et al.* (2008) EML4-ALK fusion gene and efficacy of an ALK kinase inhibitor in lung cancer. *Clin Cancer* Res 14:4275–4283.
29. Takeuchi K, *et al.* (2008) Multiplex reverse transcription-PCR screening for EML4-ALK fusion transcripts. *Clin Cancer Res* 14:6618–6624.

Respirology (2008) **13**, 646–653 doi: 10.1111/j.1440-1843.2008.01322.x

ORIGINAL ARTICLE

Preventive effects of edaravone, a free radical scavenger, on lipopolysaccharide-induced lung injury in mice

SHUNJI TAJIMA,[1,2] MANABU SODA,[1] MASASHI BANDO,[1] MUNEHIRO ENOMOTO,[1] HIDEAKI YAMASAWA,[1] SHOJI OHNO,[1] TOSHINORI TAKADA,[2] EIICHI SUZUKI,[2] FUMITAKE GEJYO[2] AND YUKIHIKO SUGIYAMA[1]

[1]*Division of Pulmonary Medicine, Department of Medicine, Jichi Medical University, Tochigi, and* [2]*Division of Respiratory Medicine, Niigata University Graduate School of Medical and Dental Sciences, Niigata, Japan*

Preventive effects of edaravone, a free radical scavenger, on lipopolysaccharide-induced lung injury in mice
TAJIMA S, SODA M, BANDO M, ENOMOTO M, YAMASAWA H, OHNO S, TAKADA T, SUZUKI E, GEJYO F, SUGIYAMA Y. *Respirology* 2008; **13**: 646–653

Background and objective: Reactive oxygen species (ROS) play an important role in the pathogenesis of acute lung injury (ALI) and pulmonary fibrosis. It was hypothesized that edaravone, a free radical scavenger, would be able to attenuate LPS-induced lung injury in mice by decreasing oxidative stress.

Methods: For the *in vivo* experiments, lung injury was induced in female BALB/c mice by the intranasal instillation of LPS. Edaravone was given by intraperitoneal administration 1 h before the LPS challenge. For the *in vitro* experiments, MH-S cells (murine alveolar macrophage cell line) were exposed to edaravone, followed by stimulation with LPS.

Results: In the LPS-induced ALI mouse model, the administration of edaravone attenuated cellular infiltration into and the concentrations of albumin, IL-6, tumour necrosis factor-α, keratinocyte-derived chemokine and macrophage inflammatory protein-2 in BAL fluid. In addition, the *in vitro* studies showed that the elevated IL-6 secretion from MH-S cells in response to LPS was significantly attenuated by co-incubation with edaravone.

Conclusions: In an experimental murine model, a free radical scavenger may prevent ALI via repression of pro-inflammatory cytokine production by lung macrophages.

Key words: acute lung injury, edaravone, free radical scavenger, LPS, pro-inflammatory cytokine, reactive oxygen species.

INTRODUCTION

Acute lung injury (ALI) and its severest form, acute ARDS, are frequent complications in critically ill patients and cause significant morbidity and mortality.[1] An initiating event (sepsis, shock, trauma, multiple transfusions, pancreatitis, etc.) leads to the activation of an acute inflammatory response on a systemic level. One of the earliest manifestations of ALI/ARDS is the activation of the pulmonary endothelium and macrophages (alveolar and interstitial), the upregulation of adhesion molecules and the production of cytokines and chemokines that induce a massive sequestration of neutrophils within the pulmonary microvasculature. These cells transmigrate across the endothelium and epithelium into the alveolar space and then release a variety of cytotoxic and pro-inflammatory compounds, including proteolytic enzymes, reactive oxygen species (ROS) and nitrogen species, cationic proteins, lipid mediators and additional inflammatory cytokines.[2] These activities perpetuate a vicious cycle by recruiting additional inflammatory cells that in turn produce more cytotoxic mediators, ultimately leading to the occurrence of profound injury of the alveolo-capillary membrane and respiratory failure. However, aside from the use of

Correspondence: Shunji Tajima, Division of Respiratory Medicine, Niigata University Graduate School of Medical and Dental Sciences, 1-757 Asahimachi-dori, Chuo-ku, Niigata 951-8510, Japan. Email: tajimash@med.niigata-u.ac.jp

Received 2 August 2007; invited to revise 12 September 2007; revised 2 December 2007; accepted 29 December 2007 (Associate Editor: Yuben Moodley).

activated protein C in a subset of ALI/ARDS patients with sepsis, specific therapies are lacking, and the cascade of events leading to ALI and ARDS, once initiated, is much less amenable to specific treatment modalities.[3] New preventive and/or therapeutic measures against ALI/ARDS are eagerly awaited.

Edaravone (3-methyl-1-phenyl-2-pyrazoline-5-one) is a potent free radical scavenger and has the antioxidant ability to inhibit lipid peroxidation.[4] It is postulated that edaravone administration might improve tissue damage induced by ROS. The protective effects of edaravone on both hemispheric embolization and transient cerebral ischaemia have already been used clinically to treat acute brain infarction in Japan.[5–7] Studies have demonstrated that edaravone prevents endotoxin-induced liver injury in rats via the suppression of pro-inflammatory cytokine production.[8,9] Ito *et al.* showed that edaravone ameliorated the lung injury induced by intestinal ischaemia/reperfusion. It decreased the neutrophil infiltration, the lipid membrane peroxidation and the expression of IL-6 mRNA in the lungs, resulting in a reduction in mortality.[10]

The purpose of this study was to investigate the anti-inflammatory effects of edaravone in LPS-induced lung injury in mice. It was hypothesized that attenuation of lipid peroxidation and/or inhibition of pro-inflammatory cytokine and chemokine activation may lead to inhibition of airway inflammation.

METHODS

Mice, cells and reagents

All mice received humane care in accordance with the Guide for the Care and Use of Laboratory Animals, published by the US National Institutes of Health (NIH publication 8523, revised 1985; http://www.nyu.edu/uawc/Forms/Guide-excerpts.pdf). The study protocol was approved by the institutional Ethics Committee. Female BALB/c mice, 6–8 weeks of age, were obtained from Japan SLC (Tochigi, Japan) and housed in the animal facility. The MH-S (murine alveolar macrophage) cells were obtained from the American Type Culture Collection (Rockville, MD, USA). LPS from *Escherichia coli* was purchased from Sigma (St Louis, MO, USA). Edaravone was obtained from Mitsubishi Pharma Corporation (Tokyo, Japan).

LPS-induced acute lung injury model

After BALB/c mice were anaesthetized by the intraperitoneal administration of 0.01 mL/g of 10% pentobarbital sodium solution (Abbott Laboratories, North Chicago, IL, USA), 100 μg/kg LPS in 60 μL saline was administered intranasally as previously described.[11] Edaravone dissolved in saline at concentrations of 1.5, 15 or 150 mg/kg or the same volume of saline was administered by a single intraperitoneal injection 1 h before LPS injection. BAL fluid (BALF) and serum were sampled 6 and 24 h after LPS treatment.

Sampling of BALF and serum

Blood samples were obtained from the right atrium of the anaesthetized mice at each time point. After centrifugation at 3000 *g* for 10 min at 4°C, the serum was frozen and stored at –80°C until assayed. BAL was performed four times through a tracheal cannula with 0.7 mL saline. In each mouse examined, approximately 2.5 mL (90%) of BALF was recovered. A 100-μL aliquot was used for the total cell count, and the remainder was immediately centrifuged at 1000 *g* for 10 min. The total cell number was counted using a haemocytometre, and cell differentiation was determined for more than 500 cells on cytocentrifuge slides with Wright–Giemsa staining. The supernatant of BALF was stored at –80°C until use.

Treatment of LPS-stimulated cells with edaravone

For the *in vitro* experiments, MH-S cells were cultured in tissue flasks incubated in 100% humidity and 5% CO_2 at 37°C in RPMI 1640 medium (Sigma, St Louis, MO) supplemented with 10% heat-inactivated fetal bovine serum (GIBCO BRL, Grand Island, NY, USA) and penicillin-streptomycin (50 mg/mL, GIBCO BRL) at 1×10^6 cells/mL. MH-S cells were then plated onto six-well, flat-bottom tissue culture plates (Becton, Dickinson and Co., Franklin Lakes, NJ, USA) at a density of 3×10^5 cells/well in RPMI 1640 medium. The medium was changed every 2 days until the cells became confluent, At this point, the cultures were washed three times with 2 mL PBS, followed by the addition of 2 mL fresh serum-free media (RPMI 1640). Cells were then treated with various concentrations of edaravone (0~100 μmol/L) for 1 h followed by incubation with 1 μg/mL of LPS or medium alone. After 3, 6 and 24 h of LPS challenge, cell-free culture supernatants were collected and stored at –80°C until assay.

Assays for cytokines and lipid hydroperoxide

The levels of pro-inflammatory cytokines, IL-6 and tumour necrosis factor-α (TNF-α) and CXC chemokines, macrophage inflammatory protein-2 (MIP-2) and keratinocyte-derived chemokine (KC), were measured in BALF, serum, and culture supernatant. The levels of IL-6 and TNF-α were measured by a sandwich ELISA kit (Biosource International, Camarillo, CA, USA). MIP-2 was measured by the Mouse MIP-2 ELISA kit (R&D Systems, Minneapolis, MN, USA). KC was measured by the Mouse KC sandwich EIA kit (Immuno-Biological Laboratories Co., Ltd., Gunma, Japan). The concentrations of lipid hydroperoxide (LPO) in serum and BALF were measured as an indicator of oxidative stress using the Lipid Hydroperoxide Assay kit (Cayman Chemical, Ann Arbor, MI, USA). The albumin concentration was determined in the cell-free BALF supernatant by dye-binding assay (Bio-Rad protein assay; Bio-Rad, Richmond, CA).

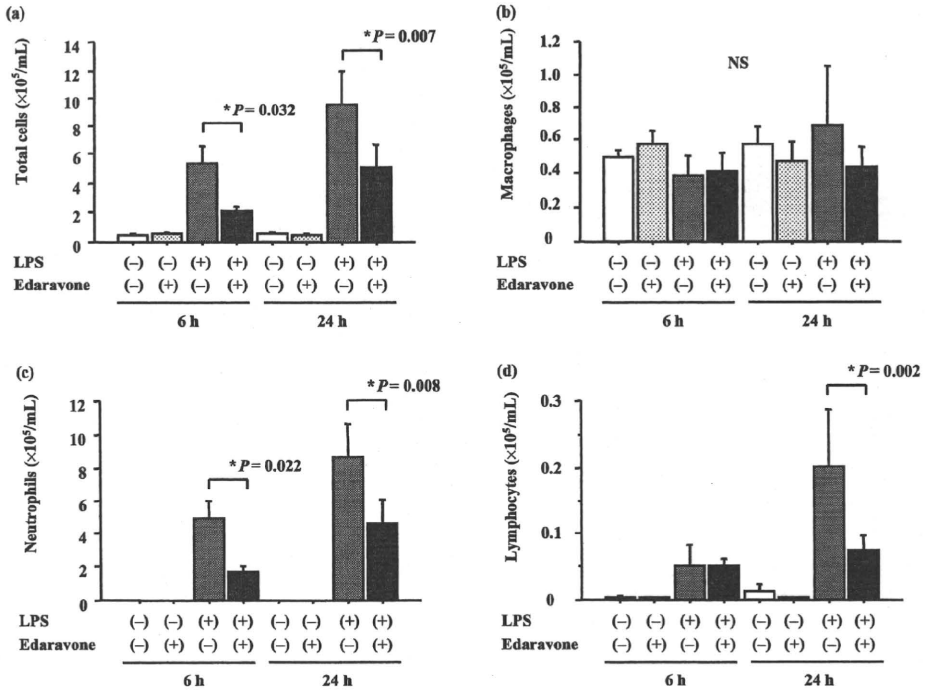

Figure 1 Effects of edaravone on the cell counts in BAL fluid (BALF) in a LPS-induced acute lung injury (ALI) mouse model (□, control group; ▨, edaravone group; ■, LPS group; ■, LPS + edaravone group). To induce ALI, LPS was instilled intranasally 1 h after the intraperitoneal administration of 150 mg/kg edaravone. The number of total cells (a) and neutrophils (c) in BALF in the LPS + edaravone group at 6 and 24 h after the LPS challenge was significantly decreased in comparison to the LPS group. At 24 h after the LPS challenge, edaravone caused a significant reduction in the number of lymphocytes (d); however, no difference was seen in the number of macrophages (b). Data are presented as mean ± SEM ($n = 6$ in each group). *$P < 0.05$ in comparison to LPS group. NS, not significant.

Statistical analysis

Data were expressed as means ± SEM. For multiple comparisons, one-way analysis of variance was used with the Fisher protected least-significant differences method used as the *post hoc* test. Differences between two variables were assessed with the Mann–Whitney *U*-test. A *P*-value < 0.05 was considered statistically significant.

RESULTS

Effects of edaravone pretreatment on BALF inflammatory cells

Pretreatment with 150 mg/kg of edaravone caused a significant reduction in inflammatory cell infiltration in BALF.

The number of total cells in BALF in the edaravone-treated mice at 6 and 24 h after the LPS challenge was significantly decreased in comparison to that in untreated mice (Fig. 1a). Similarly, the pre-administration of edaravone caused a significant reduction in the neutrophils in BALF at 6 and 24 h after the LPS challenge (Fig. 1c). At 24 h after the LPS challenge, the pre-administration of edaravone caused a significant reduction in the lymphocytes in BALF (Fig. 1d); however, no difference was seen in the BALF macrophages (Fig. 1b). Low-dose (1.5 or 15 mg/kg) edaravone did not prevent LPS-induced ALI (data not shown).

Effects of edaravone pretreatment on albumin levels in BALF

The preventive effects of edaravone on lung permeability were assessed by measurement of the albumin content in the BALF of the LPS-induced ALI model. The albumin level in BALF was significantly increased in mice given LPS, but pretreatment with 150 mg/kg edaravone significantly reduced BALF albumin levels at 6 and 24 h after LPS instillation (Fig. 2).

Effects of edaravone pretreatment on pro-inflammatory cytokine and LPO production in BALF and serum

Pro-inflammatory cytokines IL-6 and TNF-α are secreted by activated alveolar macrophages in

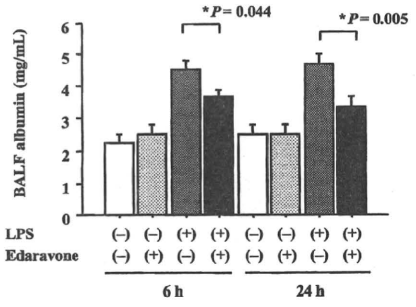

Figure 2 Effects of edaravone on albumin levels in BAL fluid (BALF) in a LPS-induced acute lung injury (ALI) mouse model (□, control group; ▨, edaravone group; ■, LPS group; ■, LPS + edaravone group). The single administration of 150 mg/kg edaravone 1 h before LPS challenge significantly reduced the BALF levels of albumin at 6 and 24 h after LPS instillation. Data are presented as mean ± SEM ($n = 6$ in each group). *$P < 0.05$ in comparison to the LPS group.

patients with ALI/ARDS.[1] The BALF levels of IL-6 (Fig. 3a) and TNF-α (Fig. 3b) peaked 6 h after LPS instillation and rapidly decreased thereafter. These elevations were significantly attenuated by 150 mg/kg edaravone administration ($P < 0.05$). The BALF levels of KC (Fig. 3c) and MIP-2 (Fig. 3d), which are chemotaxins for neutrophils similar to human IL-8, also peaked at 6 h, and the elevations were significantly attenuated by edaravone pre-administration ($P < 0.05$). Serum levels of IL-6 (Fig. 4a) and KC (Fig. 4c) showed similar profiles to the BALF levels of IL-6 and KC. They peaked at 6 h and the elevation was significantly attenuated by edaravone before administration ($P < 0.05$). No significant differences were observed in the serum levels of TNF-α (Fig. 4b) or MIP-2 (Fig. 4d). The serum and BALF levels of LPO were not decreased in mice pretreated with edaravone (data not shown).

Effects of edaravone on pro-inflammatory cytokine production from LPS-stimulated MH-S cells *in vitro*

MH-S cells were pretreated with various concentrations of edaravone (0~100 μmol/L) for 1 h and then

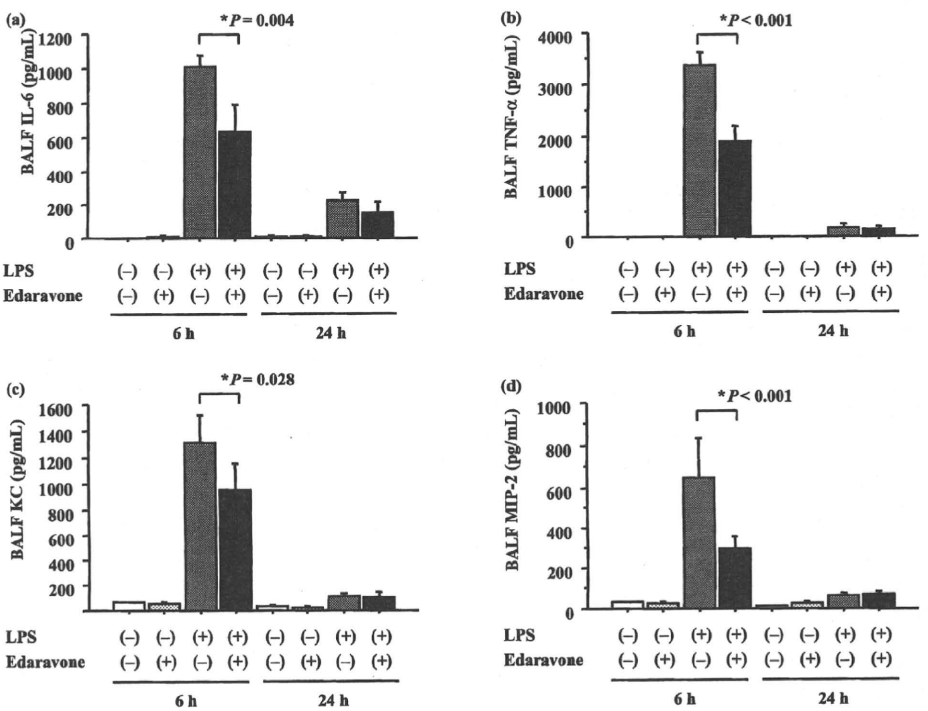

Figure 3 Effects of edaravone on pro-inflammatory cytokine production in BAL fluid (BALF) in a lioppolysaccharide (LPS)-induced acute lung injury (ALI) mouse model (□, control group; ▨, edaravone group; ■, LPS group; ■, LPS + edaravone group) To induce ALI, LPS was instilled intranasally 1 h after the intraperitoneal administration of 150 mg/kg edaravone. BALF levels of IL-6 (a), tumour necrosis factor (TNF)-α (b), keratinocyte-derived chemokine (KC) (c) and macrophage inflammatory protein-2 (MIP-2) (d) were all significantly attenuated in the LPS + edaravone group in comparison to the LPS group at 6 h after the LPS challenge. Data are presented as mean ± SEM ($n = 6$ in each group). *$P < 0.05$ in comparison to the LPS group.

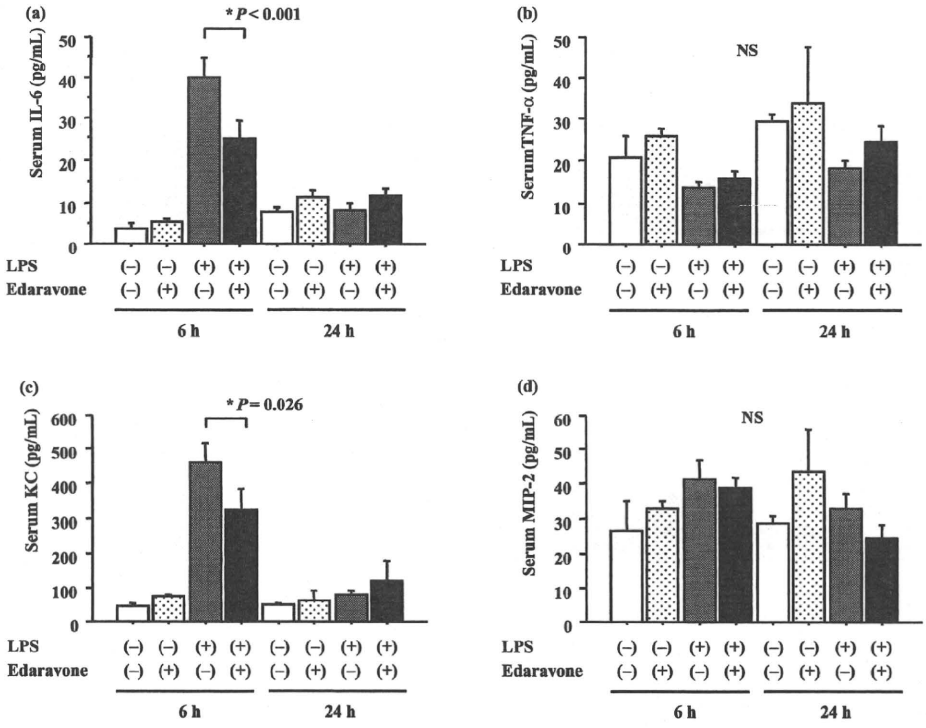

Figure 4 Effects of edaravone on pro-inflammatory cytokine production in sera in a LPS-induced acute lung injury (ALI) mouse model (□, control group; ▨, edaravone group; ■, LPS group; ■, LPS + edaravone group). To induce ALI, LPS was instilled intranasally 1 h after the intraperitoneal administration of 150 mg/kg edaravone. Although serum levels of IL-6 (a) and keratinocyte-derived chemokine (KC) (c) were significantly attenuated in the LPS + edaravone group in comparison to the LPS group, no significant differences were observed in the serum levels of tumour necrosis factor (TNF)-α (b) and macrophage inflammatory protein-2 (MIP-2) (d) among the four groups 6 h after the LPS challenge. Data are presented as mean ± SEM ($n = 6$ in each group). *$P < 0.05$ in comparison to the LPS group. NS, not significant.

were left unstimulated or stimulated with 1 μg/mL LPS for 24 h. The concentrations of IL-6, TNF-α, KC and MIP-2 in the culture supernatant were measured by ELISA. Edaravone dose-dependently inhibited IL-6 production by LPS-stimulated MH-S cells (Fig. 5a). Levels of TNF-α, KC and MIP-2 in the culture supernatant were similar in all treatment groups (Fig. 5b–d). The levels of IL-6, TNF-α, KC and MIP-2 in the culture supernatant at 3 and 6 h after LPS exposure were not attenuated by any dose of edaravone (data not shown). Furthermore, similar experiments were conducted using murine alveolar macrophages, but not cell lines, harvested by BALF, *in vitro* to determine the specific mechanics, but there was no significant difference compared with MH-S cells (data not shown).

DISCUSSION

The present study demonstrated that in the LPS-induced ALI model, edaravone attenuated cellular infiltration and concentrations of albumin, IL-6, TNF-α, KC and MIP-2 in BALF. *In vitro* studies demonstrated that elevated IL-6 secretion from MH-S cells in response to LPS was significantly attenuated by edaravone. These findings suggested that edaravone could prevent ALI via repression of cytokine release from macrophages.

Neutrophils are key players in the pathogenesis of ALI, releasing lipid, enzyme mediators and oxygen radicals.[12,13] Accumulation of neutrophils within the lung in the setting of LPS-induced stimulation probably depends on the coordinated expression of pro-inflammatory cytokines, adhesion molecules and the establishment of chemotactic gradients via the local generation of chemotactic factors. TNF-α, an early pro-inflammatory cytokine, is believed to trigger the activation of other pro-inflammatory cytokines, such as IL-6 and IL-8.[14] A sufficient concentration of edaravone for the inhibition of IL-6 from MH-S cells ranged from 10–100 μmol/L. At 5 min after a single intravenous administration of edaravone (2 mg/kg/day: roughly equivalent to the daily human dose) to male rats, edaravone levels in plasma and lung tissue were about 1 and 0.5 μmol/L, respectively.[15] To inhibit pro-inflammatory cytokine production by LPS, concentrations of edaravone 10–100 times higher than the daily human dose might be necessary. The levels of TNF-α, KC and MIP-2 in the

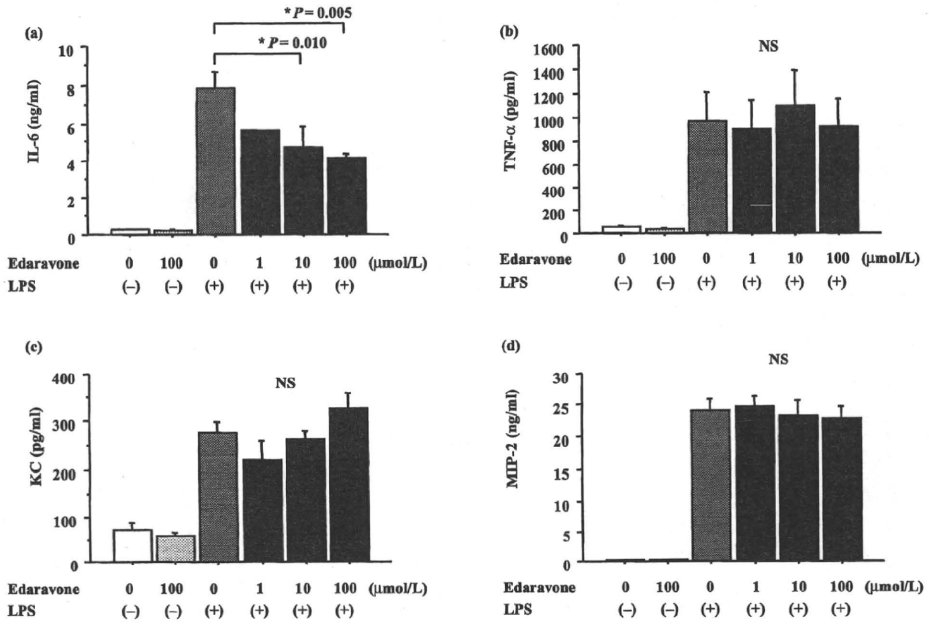

Figure 5 Effects of edaravone on pro-inflammatory cytokine production from LPS-stimulated MH-S cells *in vitro* (□, control group; ▨, edaravone group; ■, LPS group; ■, LPS + edaravone group). MH-S cells pretreated with various concentrations of edaravone (0–100 μmol/L) for 1 h were left unstimulated or stimulated with 1 μg/mL of LPS for 24 h. Treatment with edaravone significantly inhibited IL-6 production by LPS-stimulated MH-S cells, dose-dependently (a). No differences were found in tumour necrosis factor (TNF)-α, keratinocyte-derived chemokine (KC), or macrophage inflammatory protein-2 (MIP-2) levels in culture supernatants (b–d). The mean pro-inflammatory cytokine concentrations ± SEM are shown for the cumulative data from each of three samples in three independent experiments. $^*P < 0.05$ in comparison to the LPS group. NS, not significant.

culture supernatant of MH-S cells were not affected by treatment with edaravone 3, 6 or 24 h after LPS exposure. Although the reasons for the differences in the effective concentration of edaravone between *in vivo* and *in vitro* studies are not known, other cells such as neutrophils, epithelial cells, endothelial cells, dendritic cells or lymphocytes might cooperate with monocyte-macrophages at different concentrations of edaravone.

The main adverse effects of edaravone are renal failure and liver dysfunction.[15] No significant effect on heart rate or blood pressure at the dose of 450 mg/kg of edaravone was reported.[16] No adverse effects of a single administration of 150 mg/kg/day of edaravone were observed in the present study. The usual daily dose of edaravone in humans for the treatment of cerebral infarction is approximately 1.5 mg/kg, and the medication is continued for 14 days.[4–7] In the present study, LPS-induced ALI could not be prevented by a low dose (1.5–15 mg/kg/day) of edaravone. The dose of edavarone used, 150 mg/kg, was roughly 100 times the daily human dose administered as a single injection in this study. Anzai *et al.* have shown the radioprotective effect of edaravone on whole body X-ray irradiation in C3H mice.[16] An increase in the survival rate required 450 mg/kg intraperitoneally of edavarone given 30 min prior to the irradiation.[16] High-dose pulse therapy with edaravone might be needed for the prevention of lung injury induced by LPS; as it is needed to prevent injury induced by irradiation.

Edaravone is a potent-free radical scavenger and has the antioxidant ability to inhibit lipid peroxidation.[4] The amount of LPO in BALF and serum is an indicator of oxidative stress.[17] The results of the present study, however, demonstrated that the serum and BALF levels of LPO did not decrease in edaravone-treated mice. Kono *et al.* have shown that the increases in 4-hydroxynonenal (HNE)-modified protein, a cytotoxic lipid peroxidation product, were blunted in the liver by edaravone.[8] Tsuji *et al.* have shown that the elevated levels of serum malondialdehyde (MDA), which is one of the most frequently used indicators of lipid peroxidation, were inhibited significantly by edaravone administration.[9] In the present study, no inhibition of ROS production by edaravne was shown. The reasons for the discrepancy between these studies are not known, but might relate to the differences in drug delivery or transition to the liver or lung. Investigation of the indicators of lipid peroxidation without LPO, such as HNE and MDA, could determine the mechanics of anti-oxidants.

Nuclear factor-kappa B (NF-κB) is one of the crucial transcription factors required for the maximal transcription of a wide array of pro-inflammatory molecules including TNF-α and other mediators. In endotoxaemia, NF-κB freed from IκB (inhibitor κB) translocates into the nucleus, where it enhances the transcription of cytokines such as TNF-α and IL-6.[18] The pivotal role of the activation of NF-κB in inflammation during ALI has been well

elucidated in previous studies.[12,19,20] Although the mechanism of the inhibitory effects of edaravone in the inflammatory response is incompletely understood, several studies of the relationship between NF-κB and edaravone have been published.[9,21] In the pathway of activation of NF-κB, ROS are regarded as second messengers.[22,23] It has been reported that several anti-oxidants block the activation of NF-κB through the inhibition of ROS *in vitro*.[24–26] Kokura *et al.* have shown that pretreatment with edaravone scavenged the ROS and inhibited the activation of NF-κB.[21] Furthermore, Tsuji *et al.* have shown that edaravone prevented endotoxin-induced liver injury after partial hepatectomy not only by attenuating oxidative damage, but also by reducing the production of inflammatory cytokines, cytokine-induced neutrophil chemoattractant and inducible nitric oxide synthase, in part through the inhibition of NF-κB activation.[9] Although NF-κB was not examined, in the present study, it is possible that edaravone might affect the activation of NF-κB, causing the decrease of pro-inflammatory cytokine production in this LPS-induced ALI model.

In summary, the results of the present study indicated that edaravone could inhibit LPS-induced lung injury via repression of pro-inflammatory cytokine production. Clinical studies in patients with ALI/ARDS will be necessary to determine the appropriate dose, route of administration and duration of treatment.

ACKNOWLEDGEMENT

The authors thank Mrs Tomoko Ikahata, Division of Pulmonary Medicine, Department of Medicine, Jichi Medical University, for her excellent assistance. This study was supported by the Health and Labour Sciences Research Grants on Diffuse Lung Diseases from the Japanese Ministry of Health, Labour and Welfare.

REFERENCES

1 Ware LB, Matthay MA. The acute respiratory distress syndrome. *N. Engl. J. Med.* 2000; **342**: 1334–49.
2 Lee WL, Downey GP. Neutrophil activation and acute lung injury. *Curr. Opin. Crit. Care* 2001; **7**: 1–7.
3 Bernard GR, Vincent JL, Laterre PF, LaRosa SP, Dhainaut JF *et al.* Efficacy and safety of recombinant human activated protein C for severe sepsis. *N. Engl. J. Med.* 2001; **344**: 699–709.
4 Abe K, Yuki S, Kogure K. Strong attenuation of ischemic and postischemic brain edema in rats by a novel free radical scavenger. *Stroke* 1988; **19**: 480–5.
5 Kawai H, Nakai H, Suga M, Yuki S, Watanabe T *et al.* Effects of a novel free radical scavenger, MCI-186, on ischemic brain damage in the rat distal middle cerebral artery occlusion model. *J. Pharmacol. Exp. Ther.* 1997; **281**: 921–7.
6 Watanabe T, Yuki S, Egawa M, Nishi H. Protective effects of MCI-186 in cerebral ischemia: possible involvement of free radical scavenging and antioxidant actions. *J. Pharmacol. Exp. Ther.* 1994; **268**: 1597–604.
7 Wu TW, Zeng LH, Wu J, Fung KP. MCI-186: further histochemical and biochemical evidence of neuroprotection. *Life Sci.* 2000; **67**: 2387–92.
8 Kono H, Asakawa M, Fujii H, Maki A, Amemiya H *et al.* Edaravone, a novel free radical scavenger, prevents liver injury and mortality in rats administered endotoxin. *J. Pharmacol. Exp. Ther.* 2003; **307**: 74–82.
9 Tsuji K, Kwon AH, Yoshida H, Qiu Z, Kaibori M *et al.* Free radical scavenger (edaravone) prevents endotoxin-induced liver injury after partial hepatectomy in rats. *J. Hepatol.* 2005; **42**: 94–101.
10 Ito K, Ozasa H, Horikawa S. Edaravone protects against lung injury induced by intestinal ischemia/reperfusion in rat. *Free Radic. Biol. Med.* 2005; **38**: 369–74.
11 Szarka RJ, Wang N, Gordon L, Nation PN, Smith RH. A murine model of pulmonary damage induced by lipopolysaccharide via intranasal instillation. *J. Immunol. Methods* 1997; **202**: 49–57.
12 Tian J, Lin X, Guan R, Xu JG. The effects of hydroxyethyl starch on lung capillary permeability in endotoxic rats and possible mechanisms. *Anesth. Analg.* 2004; **98**: 768–74.
13 Abraham E. Neutrophils and acute lung injury. *Crit. Care Med.* 2003; **31**: S195–9.
14 Drost EM, Macnee W. Potential role of IL-8, platelet-activating factor and TNF-alpha in the sequestration of neutrophils in the lung: effects on neutrophil deformability, adhesion receptor expression, and chemotaxis. *Eur. J. Immunol.* 2002; **32**: 393–403.
15 Komatsu T, Nakai H, Masak K, Obata R, Nakai K *et al.* [Pharmacokinetic studies of 3-methyl-1phenyl-2-pyrazoline-5-one (MCI-186) in Rats (2): blood and plasma levels, distribution, metabolism, excretion and accumulation during and after repeated intravenous administration.] *Yakubutsu Dotai* 1996; **11**: 481–91 (in Japanese).
16 Meyer R, Caselmann WH, Schluter V, Schreck R, Hofschneider PH *et al.* Hepatitis B virus transactivator MHBst: activation of NF-kappa B, selective inhibition by antioxidants and integral membrane localization. *EMBO J.* 1992; **11**: 2992–3001.
17 Anzai K, Furuse M, Yoshida A, Matsuyama A, Moritake T *et al.* In vivo radioprotection of mice by 3-methyl-1-phenyl-2-pyrazolin-5-one (edaravone; Radicut), a clinical drug. *J. Rasiat. Res. (Tokyo)* 2004; **45**: 319–23.
18 Hagiwara SI, Ishii Y, Kitamura S. Aerosolized administration of N-acetylcysteine attenuates lung fibrosis induced by bleomycin in mice. *Am. J. Respir. Crit. Care Med.* 2000; **162**: 225–31.
19 Ali S, Mann DA. Signal transduction via the NF-kappa B pathway: a targeted treatment modality for infection, inflammation and repair. *Cell Biochem. Funct.* 2004; **22**: 67–79.
20 Liu SF, Ye X, Malik AB. Pyrrolidine dithiocarbamate prevents I-kappa B degradation and reduces microvascular injury induced by lipopolysaccharide in multiple organs. *Mol. Pharmacol.* 1999; **55**: 658–67.
21 Lim CM, Kim EK, Koh Y, Kim WS, Kim DS *et al.* Hypothermia inhibits cytokine release of alveolar macrophage and activation of nuclear factor kappa B in endotoxemic lung. *Intensive Care Med.* 2004; **30**: 1638–44.

22 Kokura S, Yoshida N, Sakamoto N, Ishikawa T, Takagi T *et al.* The radical scavenger edaravone enhances the anti-tumor effects of CPT-11 in murine colon cancer by increasing apoptosis via inhibition of NF-kappa B. *Cancer Lett.* 2005; **229**: 223–33.
23 Schreck R, Rieber P, Baeuerle PA. Reactive oxygen intermediates as apparently widely used messengers in the activation of the NF-kappa B transcription factor and HIV-1. *EMBO J.* 1991; **10**: 2259–66.
24 Sen CK, Packer L. Antioxidant and redox regulation of gene transcription. *FASEB J.* 1996; **10**: 709–20.
25 Schreck R, Meier B, Maennel DN, Droge W, Baeuerle A. Dithio-carbamates as potent inhibitors of nuclear factor kB activation in intact cells. *J. Exp. Med.* 1992; **175**: 1181–94.
26 Suzuki YJ, Aggarwal BB, Packer L. Alpha-lipoic acid is potent inhibitor of NF- kappa B activation in human T cells. *Biochem. Biophys. Res. Commun.* 1992; **189**: 1709–15.

European Respiratory Society

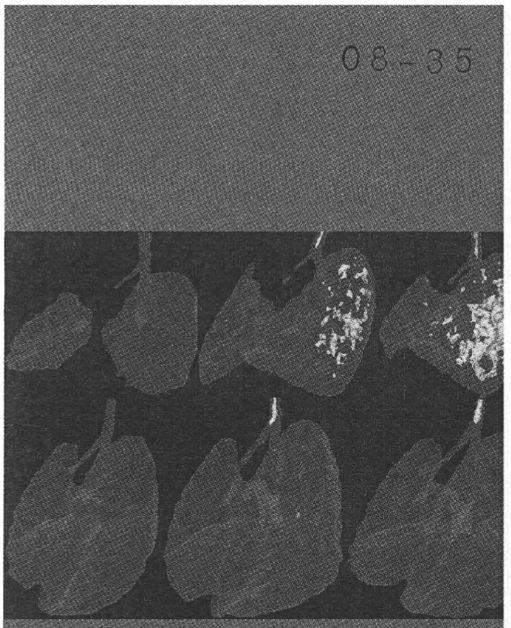

European Respiratory Journal

www.erj.ersjournals.com

Eur Respir J 2008; 32: 1337–1343
DOI: 10.1183/09031936.00164407

Effects of edaravone, a free-radical scavenger, on bleomycin-induced lung injury in mice

S. Tajima*,#, M. Bando*, Y. Ishii*, T. Hosono*, H. Yamasawa*, S. Ohno*, T. Takada#, E. Suzuki#, F. Gejyo# and Y. Sugiyama*

ABSTRACT: Reactive oxygen species play an important role in the pathogenesis of acute lung injury and pulmonary fibrosis. The present authors hypothesise that edaravone, a free-radical scavenger, is able to attenuate bleomycin (BLM)-induced lung injury in mice by decreasing oxidative stress.

Lung injury was induced in female ICR mice by intratracheal instillation of 5 mg·kg^{-1} of BLM. Edaravone (300 mg·kg^{-1}) was administered by intraperitoneal administration 1 h before BLM challenge.

Edaravone significantly improved the survival rate of mice treated with BLM from 25 to 90%, reduced the number of total cells and neutrophils in bronchoalveolar lavage fluid (BALF) on day 7, and attenuated the concentrations of lipid hydroperoxide in BALF and serum on day 2. The fibrotic change in the lung on day 28 was ameliorated by edaravone, as evaluated by histological examination and measurement of hydroxyproline contents. In addition, edaravone significantly increased the prostaglandin E_2 concentration in BALF on day 2.

In summary, edaravone was shown to inhibit lung injury and fibrosis *via* the repression of lipid hydroperoxide production and the elevation of prostaglandin E_2 production in the present experimental murine system.

KEYWORDS: Bleomycin, edaravone, free-radical scavenger, lung injury, pulmonary fibrosis

Idiopathic pulmonary fibrosis (IPF) is defined as a specific form of chronic fibrosing interstitial pneumonia limited to the lung [1]. The aetiology of IPF is not known, and IPF remains a devastating disease with a 5-yr mortality rate of >50% [1]. Unfortunately, the pathogenesis of IPF is also incompletely understood. Although several drugs have been used or tested for IPF, there is no established treatment that definitely improves its outcome [1]. Thus, new therapies are awaited, based on new understanding of the pathogenesis of IPF. There is considerable evidence that oxygen-generated free radicals play a major role in inflammatory and immune-mediated tissue injury [2–4]. DEMEDTS *et al.* [5] have shown that acetylcysteine, a precursor of the major antioxidant glutathione, administered at a daily dose of 1,800 mg in combination with prednisone and azathioprine, preserves vital capacity and carbon monoxide diffusing capacity better in patients with IPF than the combination of prednisone and azathioprine alone. These findings suggest that an oxidant–antioxidant imbalance may contribute to the disease process in IPF.

Bleomycin (BLM), an antineoplastic agent, induces pulmonary fibrosis as an adverse effect, since the hydrolase that inactivates BLM is relatively scarce in lung tissue. The mechanism of the antineoplastic effect of BLM is that the BLM-iron complex reduces molecular oxygen to superoxide and hydroxy radicals that can then attack DNA and cause strand cleavage [6]. The role of oxygen free radicals has been supported by studies showing that the addition of superoxide dismutase, an oxygen free-radical scavenger, inhibited BLM-induced DNA breakage and cellular damage *in vitro* [7–10]. Therefore, a BLM-induced pulmonary fibrosis model in mice is a helpful tool to examine the general mechanism of fibrosis, especially the mechanism mediated by oxygen free radicals.

Edaravone (3-methyl-1-phenyl-2-pyrazolin-5-one) is a potent free-radical scavenger and has the antioxidant ability to inhibit lipid peroxidation [11]. Therefore, it is speculated that edaravone administration might ameliorate the tissue damage induced by reactive oxygen species (ROS).

AFFILIATIONS
*Division of Pulmonary Medicine, Dept of Medicine, Jichi Medical University, Shimotsuke, and #Division of Respiratory Medicine, Niigata University Graduate School of Medical and Dental Sciences, Niigata, Japan.

CORRESPONDENCE
S. Tajima
Division of Respiratory Medicine
Niigata University Graduate School of Medical and Dental Sciences
1-757 Asahimachi-dori
Chuo-ku
Niigata
951-8510
Japan
Fax: 81 252270775
E-mail: tajimash@med.niigata-u.ac.jp

Received:
December 06 2007
Accepted after revision:
July 02 2008

SUPPORT STATEMENT
This study was supported by the Health and Labour Sciences Research Grants on Diffuse Lung Diseases from the Japanese Ministry of Health, Labour and Welfare.

STATEMENT OF INTEREST
A statement of interest for this study can be found at www.erj.ersjournals.com/misc/statements.shtml

European Respiratory Journal
Print ISSN 0903-1936
Online ISSN 1399-3003

Edaravone has protective effects on both hemispheric embolisation and transient cerebral ischaemia, and has, therefore, been used clinically to treat acute brain infarction in Japan [12–14]. ITO *et al.* [15] have shown that edaravone ameliorated the lung injury induced by intestinal ischaemia/reperfusion. In the study by ITO *et al.* [15], edaravone decreased the neutrophil infiltration, the lipid membrane peroxidation and the expression of interleukin (IL)-6 mRNA in the lungs, resulting in a reduction in mortality. Most recently, ASAI *et al.* [16] have shown that edaravone suppressed BLM-induced acute pulmonary injury in rabbits. They reported that a 10-day intravenous edaravone administration beginning 3 days prior to intratracheal instillation of BLM significantly attenuated the acute BLM-induced lung injury and the numbers of both terminal deoxynucleotidyltransferase-mediated deoxyuridine triphosphate-positive (apoptotic) and transforming growth factor-β positive cells on day 7 [16]. Although the results of ASAI *et al.* [16] support the present authors' hypothesis, it was thought that several critical points were lacking, as follows: 1) collagen accumulation at the late fibrosing stage was not evaluated; and 2) bronchoalveolar lavage (BAL) was not performed and ROS was not measured in order to evaluate inhibitory effects on the inflammatory process. Accordingly, in the present study, a BLM-induced pulmonary fibrosis model was used in mice, which is a more common animal lung fibrosis model than the rabbit model used by ASAI *et al.* [16], to investigate the ability of edaravone to: 1) inhibit pulmonary fibrosis; or 2) decrease lung inflammation and attenuate ROS.

MATERIALS AND METHODS

Mice, cells and reagents

All mice received humane care in accordance with the Guide for the Care and Use of Laboratory Animals, US National Institutes of Health (Bethesda, MD, USA). The study protocol was approved by the Ethics Committee of Jichi Medical University (Tochigi, Japan). Female ICR mice, 6–8 weeks of age, were obtained from Japan SLC (Tochigi, Japan) and housed in the animal facility of Jichi Medical University. BLM was purchased from Nippon Kayaku (Tokyo, Japan). Edaravone was a gift from Mitsubishi Pharma Corporation (Tokyo, Japan). It was dissolved in a small amount of 1 N NaOH solution, the pH was adjusted to 7.0 with 1 N HCl and the concentration was adjusted to 3 $mg \cdot mL^{-1}$ in the saline solution.

BLM-induced pulmonary fibrosis model

To induce pulmonary fibrosis, ICR mice were treated with intratracheal BLM on day 0. The ICR mice were anaesthetised by the intraperitoneal administration of 0.01 $mL \cdot g^{-1}$ of 10% pentobarbital sodium solution (Abbott Laboratories, North Chicago, IL, USA), followed by intratracheal instillation of 5 $mg \cdot kg^{-1}$ body weight of BLM in 50 μL of sterile isotonic saline. The control animals received intratracheal saline only. Edaravone dissolved in saline or the same volume of saline was administered by a single intraperitoneal injection either 1 h before or 24 h after BLM injection. To ascertain the optimal dose of edaravone for the proposed experiment, mice were given edaravone at a dose of 0, 3, 30 or 300 $mg \cdot kg^{-1}$ or the same volume of saline (10–12 mice in each group). The mice were killed under anaesthesia on day 2, 7 or 28 after BLM instillation, for examination. On day 28, the left lung lobes were used for hydroxyproline assay. In the mice receiving pre-administration of 300 $mg \cdot kg^{-1}$ edaravone with BLM instillation, BAL was performed on days 2 and 7. In addition, histological examination was performed on day 28. The present authors randomly selected six or 10 mice samples from each group. Mortality calcuation, hydroxyproline assay, histological examination and BAL analysis were performed independently.

Sampling of BAL fluid and serum

Under anaesthesia, as previously described, blood samples were obtained from the right atrium at each time-point. After centrifugation at 3,000 × *g* for 10 min at 4°C, the serum was frozen and stored at -80°C until it was assayed. BAL was performed four times through a tracheal cannula with 0.7 mL of saline. In each mouse examined, ~2.5 mL (90%) of BAL fluid (BALF) was recovered. A 100-μL aliquot was used for the total cell count, and the remainder was immediately centrifuged at 1,000 × *g* for 10 min. The total cell count was prepared using a haemocytometer, and cell differentiation was determined for >500 cells on cytocentrifuge slides with Wright–Giemsa staining. The supernatants of BALF were stored at -80°C until used.

Morphological evaluation

Histopathological evaluation was performed on day 28 in the BLM-induced pulmonary fibrosis model. Both lungs were removed and inflated with 10% formaldehyde neutral buffer solution, and longitudinal tissue sections were stained with haematoxylin and eosin.

Assay of hydroxyproline

Hydroxyproline in the murine lung on day 28 after BLM instillation was assayed according to the commonly used

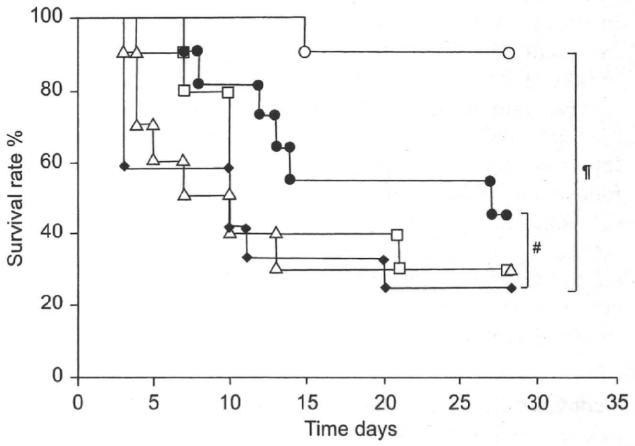

FIGURE 1. Effects of edaravone on mortality in a bleomycin (BLM)-induced lung injury mouse model. The survival rates of five study groups of mice are shown over a 28-day observation period (10–12 mice in each group). The four BLM + edaravone groups received single intraperitoneal infusion of edaravone as follows. ○: high dose of edaravone (pre-treatment, 300 $mg \cdot kg^{-1}$); □: intermediate dose of edaravone (pre-treatment, 30 $mg \cdot kg^{-1}$); △: low dose of edaravone (pre-treatment, 3 $mg \cdot kg^{-1}$) administered as a single intraperitoneal infusion 1 h before the instillation of BLM; ●: high dose of edaravone as a single intraperitoneal infusion 24 h after the instillation of BLM (treatment, 300 $mg \cdot kg^{-1}$). The survival rate of the high-dose edaravone group (pre-treatment, 300 $mg \cdot kg^{-1}$; ○) was significantly higher than the group administered intratracheal instillation of BLM (♦; $p<0.05$). The results for the control group are not shown. #: $p=0.15$; ¶: $p=0.002$.